

Dynamic Loading of Substation Distribution Transformers: An Application for use in a
Production Grade Environment

by

Ming Zhang

A Thesis Presented in Partial Fulfillment
of the Requirements for the Degree
Master of Science

Approved October 2013 by the
Graduate Supervisory Committee:

Daniel J. Tylavsky, Chair
Raja Ayyanar
Keith Holbert

ARIZONA STATE UNIVERSITY

December 2013

ABSTRACT

Recent trends in the electric power industry have led to more attention to optimal operation of power transformers. In a deregulated environment, optimal operation means minimizing the maintenance and extending the life of this critical and costly equipment for the purpose of maximizing profits. Optimal utilization of a transformer can be achieved through the use of dynamic loading. A benefit of dynamic loading is that it allows better utilization of the transformer capacity, thus increasing the flexibility and reliability of the power system. This document presents the progress on a software application which can estimate the maximum time-varying loading capability of transformers. This information can be used to load devices closer to their limits without exceeding the manufacturer specified operating limits.

The maximally efficient dynamic loading of transformers requires a model that can accurately predict both top-oil temperatures (TOTs) and hottest-spot temperatures (HSTs). In the previous work, two kinds of thermal TOT and HST models have been studied and used in the application: the IEEE TOT/HST models and the ASU TOT/HST models. And, several metrics have been applied to evaluate the model acceptability and determine the most appropriate models for using in the dynamic loading calculations.

In this work, an investigation to improve the existing transformer thermal models performance is presented. Some factors that may affect the model performance such as improper fan status and the error caused by the poor performance of IEEE models are discussed. Additional methods to determine the reliability of transformer thermal models using metrics such as time constant and the model parameters are also provided.

A new production grade application for real-time dynamic loading operating purpose is introduced. This application is developed by using an existing planning application, TTeMP, as a start point, which is designed for the dispatchers and load specialists. To overcome the limitations of TTeMP, the new application can perform dynamic loading under emergency conditions, such as loss-of transformer loading. It also has the capability to determine the emergency rating of the transformers for a real-time estimation.

ACKNOWLEDGEMENTS

First and foremost, I would like to express my special gratitude to my advisor, Dr. Daniel J. Tylavsky, for giving me the opportunity to work on this research. I sincerely appreciate him for his invaluable guidance on this research work and assistance in completing my dissertation. His encouragement and inspiration helped me go through the tough time in my graduate study and life. His responsibility towards his students and his dedication to profession impressed me a lot.

I would like to thank my committee members, Dr. Raja Ayyanar and Dr. Keith Holbert for their valuable time and suggestions.

In addition, I would like to express my appreciation to Salt River Project, for providing financial support and supplying the data and industrial guidance. I am very grateful to the following engineers at SRP for their important and insightful contributions to this work: Ken Alteneder, Kenneth E. Brown, Jason Gunawardena, Wesley B. Knuth, Thomas W. LaRose, Gary A. McCulla, Sam Ortega and Dustin J. Stapp.

Finally, I would like to thank my parents, for supporting me financially and emotionally through my educational process. I am deeply indebted for their encouragement and motivation. And, to all my friends I met here in Arizona State University, I am grateful for their always standing by me when I need them.

TABLE OF CONTENTS

	Page
LIST OF TABLES	viii
LIST OF FIGURES	ix
NOMENCLATURE	xi
CHAPTER	
1 INTRODUCTION	1
1.1 Introduction.....	1
1.2 Research Objective	3
1.3 Literature Review.....	4
1.3.1 TOT Models	4
1.3.2 HST Models	6
1.3.3 Other Notable Research on Thermal Models	7
1.4 Summary of Chapters	8
2 SELECTED TRANSFORMER THERMAL MODELS	9
2.1 Introduction.....	9
2.2 IEEE TOT Model (Top-Oil Rise Model).....	9
2.3 IEEE HST Model (Winding Hot-Spot Rise Model).....	12
2.4 ASU TOT Model (Top-Oil Model)	15
2.5 ASU HST Model (Modified HST Model)	16
2.6 Linear Regression and the Least-Squares Method.....	17
2.7 Metrics for Model Reliability Assessment	19
2.7.1 Maximum Steady-State Load (SSL_{Max}) and Bootstrapping.....	20

CHAPTER	Page
2.7.2	Variance Inflation Factors (VIF)..... 22
2.7.3	Coefficient of Determination R^2 22
2.8	Conclusions..... 23
3	IMPROVING MODEL PERFORMANCE..... 24
3.1	Introduction..... 24
3.2	Cooling Modes..... 24
3.3	Improper fan status 26
3.4	Bad Performance of the IEEE Models..... 28
3.5	Improving Model Performance..... 30
3.6	Results of Model Performance..... 31
3.6.1	Highline3 Transformer 31
3.6.2	Kirk2 Transformer..... 33
3.7	Conclusions..... 35
4	ADDITIONAL CRITERIA FOR MODEL SELECTION 36
4.1	Introduction..... 36
4.2	Model Testing on Webber3 36
4.2.1	Simulation Results for 8/20/2009: 37
4.2.2	Simulation Results for 8/20/2009..... 39
4.2.3	Overall conclusion: 40
4.3	Additional Metrics for Model Selection 41
4.3.1	Time Constant 41
4.3.2	Other Criterion for Model Screening 43

CHAPTER	Page
4.4	Conclusion 44
5	THE APPLICATION AND GUI DESIGN 45
5.1	Introduction..... 45
5.2	The Program Design 46
5.2.1	Function Design 46
5.2.2	Directory Structure and Data Files..... 47
5.2.3	Flow Chart..... 48
5.3	GUI Design 51
5.3.1	Startup Interface 51
5.3.2	Main User Interface and Functional Area 51
5.3.3	Input Area..... 52
5.3.4	Output Area..... 55
5.4	Conclusion 57
6	DYNAMIC LOADING ALGORITHM DESIGN 58
6.1	Introduction..... 58
6.2	Definition of Dynamic Loading..... 58
6.3	Dynamic Loading Calculation for a 48-Hour Cycle..... 59
6.4	Select “The Most Similar Day” 62
6.5	Quasi-Newton Method and Binary Search Algorithm..... 63
6.6	Cooling Mode Transition in the HST and TOT Calculations..... 67
6.7	An Example of Dynamic Loading Calculation for Broadway4 Transformer 67

CHAPTER	Page
6.8 Conclusion	70
7 CONCLUSIONS AND FUTURE WORK.....	71
7.1 Conclusions.....	71
7.2 Future Work.....	72
REFERENCES	73

LIST OF TABLES

Table		Page
2.1	Values of the exponent n for different cooling modes	11
2.2	Values of the exponent m for different cooling modes	13
3.1	Estimated model parameters based on cooling mode set-point vector (75, 75, 60, 60)°C	30
3.2	Estimated model parameters based on cooling mode set-point vector (65, 75, 70, 60)°C	30
4.1	Time constant for 15 transformers	42

LIST OF FIGURES

Figure	Page
2.1 Flowchart of bootstrapping.....	21
3.1 Tier division.....	26
3.2 Fan status of the transformer DV10	27
3.3 Prediction results of Highline3 on 2009-7-20: tier-1 and tier-2 use IEEE models, tier-3 use ASU models.....	29
3.4 Prediction results of Highline3 on 2009-7-20: tier-1 and tier-2 use IEEE models, tier3 use ASU models, with TOT alone initialized to the measured TOT value at tier-2-tier-3 boundary	29
3.5 TOT prediction for 5 hottest days for transformer Highline3: (a) cooling mode set-point vector (75, 75, 60, 60)°C; (b) cooling mode set-point vector (65, 75, 70, 60)°C	32
3.6 Predicted TOT and HST on 2009-7-27 for transformer Highline3: (a) cooling mode set-points (75, 75, 60, 60)°C; (b) cooling mode set-points (65, 75, 70, 60)°C	33
3.7 TOT prediction for 5 hottest days for transformer Kirk2: (a) cooling mode set- points (75, 75, 60, 60)°C; (b) cooling mode set-points (65, 75, 70, 60)°C	34
3.8 Predicted Data on 2009-7-17 for transformer Kirk2: (a) cooling mode set-points (75, 75, 60, 60)°C; (b) cooling mode set-points (65, 75, 70, 60)°C	35
4.1 Measured and predicted data for 2009-8-20 (case 1)	38
4.2 Measured and predicted data for 2009-8-20 (case 2)	38

Figure	Page
4.3 Measured and predicted data on 2009-8-21 (case 1).....	39
4.4 Measured and predicted data on 2009-8-21 (case 2).....	40
4.5 Time constant for 15 transformers	43
5.1 Directory structure of the DLTA.....	48
5.2 The overall flowchart of the program.....	50
5.3 Startup Interface	51
5.4 Main User interface	52
5.5 Select a substation	53
5.6 Select a transformer.....	54
5.7 Enter either MVA increment or enhanced load duration	54
5.8 Other input.....	55
5.9 Dynamic loading calculation results	56
5.10 Predicted load, TOT and HST curves.....	57
6.1 The flow chart of dynamic loading calculation.....	61
6.2 Peak HST and Peak TOT versus Load Increment.....	65
6.3 Peak HST and Peak TOT versus Enhanced Duration	66
6.4 Dynamic loading of Broadway4 transformer	68
6.5 Dynamic loading result of Broadway4 transformer using IEEE model.....	69
6.6 Dynamic loading result of Broadway4 transformer using ASU model	69

NOMENCLATURE

C	Thermal capacity of transformer (Wh/ °C)
C_{jj}	The j^{th} diagonal element of the matrix $(\mathbf{X}^T \mathbf{X})^{-1}$
FA, ONAF	Oil-natural-air-forced cooling mode
FOA, OFAF	Oil-forced-air-forced cooling mode
HST	Hottest-spot temperature (°C)
HST_{max}	Maximum acceptable HST (°C)
I	Load under consideration (kVA or A)
I_{hst}	Peak value of load curve estimated based on HST
I_{oil}	Peak value of load curve estimated based on TOT
I_{rated}	Rated load (kVA or A)
I_{pu}	Ratio of specified load to rated load (per unit)
IEEE	Institute of Electrical and Electronics Engineer
k	Time step index
k_1, k_2	Weight coefficients
K_1, K_2, K_3	ASU TOT model parameters
L_{1m}, L_2	ASU HST model parameters

m	Winding hottest-spot cooling exponent
n	Top oil cooling exponent
OA, ONAN	Oil-natural-air-natural cooling mode
r	Number of regressor variables
R	Ratio of load loss to no-load loss at rated load
R^2	Coefficient of determination
SDTDL	Substation Distribution Transformer Dynamic Loading
SS_{Res}	Error sum of squares
SS_T	Measure of total variation in the observations
SSL_{Max}	Maximum steady-state load
SRP	Salt River Project
t	Time duration of load (hours)
T_{amb}	The ambient temperature (°C)
T_h	Winding time constant at hottest-spot location (min)
T_{max}^f, T_{min}^f	Highest and lowest forecast ambient temperatures
$T_{max,i}, T_{min,i}$	Highest and lowest ambient temperatures in the i th day of historical data
TOT	Top-oil temperature (°C)

TOT_{\max}	Maximum acceptable TOT (°C)
VIF	Variance inflation factors
x	Predictor or regressor variable in a regression model
\mathbf{X}	An n by p matrix containing the k regressor variables at all observation levels and extra column of all 1s
x_{ij}	Value of regressor variable x_j at the i^{th} observation
x_j	The j^{th} regressor variable
y	Response variable in a regression model
y_i	Measured value of the response variable at the i^{th} observation
\mathbf{y}	An n by 1 vector of the response variable y_i
β	Linear regression coefficient or model parameter
β_j	The j^{th} linear model parameter
$\boldsymbol{\beta}$	A p by 1 vector of linear model parameters
Δt	Sampling period
ΔT_{adjust}	Calibration temperature
ε	Error term of a regression model
$\boldsymbol{\varepsilon}$	An n by 1 vector of the error terms
θ_{amb}	Ambient temperature variation (°C)

θ_{fl}	Top-oil rise over ambient temperature at rated load (°C)
θ_h	Hottest-spot temperature rise over top-oil temperature (°C)
θ_{hi}	Initial hottest-spot temperature rise over top-oil temperature (°C)
θ_{hr}	Hottest-spot temperature rise over top-oil temperature at rated load (°C)
θ_{hst}	Hottest-spot temperature (HST) (°C)
θ_{hsti}	Initial hottest-spot temperature (°C)
θ_{hu}	Ultimate hottest-spot temperature rise over top-oil temperature (°C)
θ_i	Initial top-oil rise over ambient temperature for t=0 (°C)
θ_o	Top-oil rise over ambient temperature (°C)
θ_{oil}	Top-oil temperature (TOT) (°C)
θ_{oili}	Initial top-oil temperature (°C)
θ_u	Ultimate top-oil rise over ambient temperature rise (°C)
τ_{oil}	Oil time constant for any load and for any specific top-oil temperature rise (hours)
$\tau_{oil,R}$	Oil time constant at rated kVA (hours)
σ^2	The assumed constant variance of the error term ε

CHAPTER 1

INTRODUCTION

1.1 Introduction

Due to economic reasons, there is an increasing emphasis on improving transformer utilization to obtain maximum benefit. By increasing the maximum energy delivered each day from substation distribution transformers while keeping the loss of life within reasonable limits, utilities can save millions of dollars. To meet this object, transformers must be optimally utilized based on prevailing environmental and apparatus conditions.

Maximizing the return on an investment (ROI) in a transformer takes many factors into account, but one important tradeoff is between loading a transformer more heavily to defer capital cost versus prolonging its service life time through lighter loads. Insulation loss-of-life is the most reliable indicator of the remaining life expectancy of a transformer. Loss of insulation life is determined by the insulation temperature. Because the loading on transformers varies during the day and the response of oil and insulation temperatures lag applied load, transformers can be loaded for a “short” time with a load greater than their design/name-plate rating.

Optimal utilization of a transformer can be achieved through the use of dynamic loading. Dynamic loading is the term used for loading a transformer while taking into account the time variation of load, rule-of-thumb maximum allowable insulation temperatures, thermal time constants, cooling mode transitions and ambient temperatures.

Ultimately, insulation temperature rises because of no-load and load losses that produce heat. In oil-immersed transformers, the most frequently used thermal limits are top-oil temperature (TOT) and hottest-spot temperature (HST). In the past, the

information of hottest-spot temperature can only be acquired from conventional heat run tests which were performed after the transformer was manufactured. But the location of hottest-spot temperature was hard to determine. Recently, various methods have been suggested for direct measurements of hottest-spot temperature in transformer windings, such as fiber-optic sensors and fluoro-optic thermometers. The optimal location of these sensors has also been demonstrated. Typically, HST is the criterion which limits the maximum dynamic load profile, but when the load profile is relatively flat, TOT will be the limiting criterion. Both temperatures are usually considered when performing dynamic loading calculation.

To minimize the risk of failure and to estimate the remaining life of the transformer realistically, both top-oil temperature and hottest-spot temperature should be controlled within certain ranges. Therefore, it is necessary when performing dynamic loading to estimate TOT and HST to as high of a degree of accuracy as possibly. Much work has been done to develop accurate thermal models of the TOT and HST for substation-distribution and power transformers. An approach that involves developing superior models and then estimating the parameters of these models from measured field data has been shown to give better prediction performance [1]-[5]. The advantage comes from the fact that models derived from measured data naturally account for the unique environmental conditions of each transformer, and also account for many phenomena that develop in operating transformers, such as fouled heat exchangers and malfunctioning pumps/fans [5].

Dynamic loading simulates the thermal behavior of the transformer for the purpose of computing how heavily and how long the transformer can be loaded above the name-

plate to reach the maximum permissible TOT or HST temperatures for a given loading condition. This information can be used for load planning and scheduling purposes, allowing better utilization of the transformer capability, and increasing the flexibility of the power system operation.

1.2 Research Objective

Salt River Project (SRP) has been interested in a software application which could be used to perform dynamic loading of substation distribution transformer for load planning and scheduling. In the previous work [1]-[5], the application developed by a team at Arizona State University is capable of reading in measured data, building thermal models with historical data for transformers; then, selecting the “best” model and using the model to estimate the maximum dynamic load the transformer can sustain without violating its thermal limits. In the previously developed application, the dynamic loading calculation is performed based on the assumption that there is no change in load shape (load is added to base-case load curve equally at all the time points of a full day). This limitation of the function makes the application able to be used for planning purposes, but may not work well for emergency conditions where there is a step change to the load that is temporary.

Therefore, the objective of this research is to enhance the dynamic loading function for real-time operating purposes and develop a production grade application for both the planning and operating engineers at SRP to perform dynamic loading.

1.3 Literature Review

Improving the utilization of transformers requires that both top-oil temperature and hottest-spot temperature are predicted accurately. In the literature, the development of an HST model presumes the existence on a TOT model since the HST is a function of TOT.

The top-oil and hottest-spot thermal models given in the IEEE Guide for Loading Mineral-Oil-Immersed Transformers [6], which are commonly referred to as IEEE Clause 7 models in the literature, are widely used in industry for predicting TOT and HST. All of the parameters needed for these models can be easily distilled from the transformer heat-run test report. The IEEE TOT model assumes that all changes in top-oil temperature rise over ambient temperature are caused by changes in the load (current). However, the effect of ambient temperature variation on the changes in top-oil temperature is not properly taken into account. Therefore, the IEEE Clause 7 models, despite having a long history of acceptable performance, are criticized for their accuracy.

A substantial amount of work has been done to develop and improve the transformer thermal models. In the following section, some of the newer, more accurate TOT and HST models are discussed.

1.3.1 TOT Models

In [7], a modified version of the IEEE Clause 7 TOT model which better characterizes both loading and ambient temperature variations was developed. This model is referred to as the top oil model. The field verification of the model provided in [7] shows that the modified model does capture some phenomena that the IEEE model does not and therefore gives a significant improvement in the TOT prediction.

In [8], Swift developed a thermal model for TOT based on heat transfer theory and the thermal-electrical analogy. A simple equivalent circuit is used to represent the thermal heat flow equations for power transformers. Key features are the use of a current source analogy to represent heat input due to losses (copper and iron), and a nonlinear resistor analogy to represent the effect of air or oil cooling convection currents. Parameters in the circuit can be calculated with data obtained from heat-run tests and online monitoring devices. The field verification of the model proposed in [8] is presented in [9], showing that this thermal model adequately predicts the top-oil temperature.

A generalized TOT model for power transformers based on the basic approach proposed by Swift in [8] is developed in [10]. This method focuses specifically on the nonlinear thermal resistance of the transformer oil, where the variation in oil viscosity and winding resistance with temperature are considered. It was shown that this thermal model yields results that agree with measured values with good accuracy.

Companion papers [11] and [12] compared the performance of the TOT equations developed in [6] [7] [8] and [10] to each other. It defines metrics to measure model adequacy, accuracy and consistency and then ranks these models according to their acceptability. It was shown that, the linearized TOT model of [7] has the best performance among all the four models.

Some other TOT models contained in [13]-[15] requires some parameters that are not generally available to utilities. Therefore, these models are not suitable for this work. Of the many models available, the linearized model given in [7] was chosen for this work.

1.3.2 HST Models

Swift did not develop a model for HST in [8], but stated that an HST equation could be derived by analogy from the TOT equation presented. This suggested HST model is developed and tested in [16]. Experimental results show that the model can reflect thermal behavior of transformer well under constant loading and dynamic loading. Reference [10] contains an HST model that accounts for the nonlinear thermal resistance of the transformer oil.

In [1], the modified Clause 7 HST model from [2], the HST model by Susa in [10] and the suggested HST model in [8] are examined and compared with each other. The investigation fits the models to measured field data using numerical and statistical methods. The reliability and acceptability of these models for HST prediction are evaluated. It is shown that the modified HST model and Susa's model are acceptable for training models from field data. Swift's model is not acceptable because it is structurally deficient.

The Clause 7 model in [6] assumes that the oil temperature in the cooling ducts is the same as the tank top oil during overloads. However, an investigation reported by Pierce in [13] shows that during overloads, the temperature of the oil in the winding cooling ducts rises rapidly, and there is a time lag between the top-oil temperature rise and the oil temperature rise in the winding cooling ducts. This phenomenon results in actual winding hottest-spot temperature greater than that predicted by the Clause 7 model. In another paper [14], Pierce developed improved loading equations which consider type of liquid, cooling mode, winding duct oil temperature rise, resistance and viscosity changes, and ambient temperature and load changes during a load cycle. These equations are referred

to as Annex G equations in the literature and are included in annex G of [6]. Although with more accuracy in predicting HST, Pierce's model requires the use of bottom-oil temperature and other transformer parameters that are not normally available in the transformer test report.

A linearized HST model was derived by analogy with the linearized TOT model given in [2]. This linearized HST model was found to have good prediction performance, and, thus, is selected for use in this work.

1.3.3 Other Notable Research on Thermal Models

References [3]-[5] show that the models derived from field-measured data give better prediction performance than those using parameters obtained from transformer heat-run-test reports. The superiority comes from the fact that models trained from measured data are able to capture the unique environmental conditions and many phenomena in operating transformers. This approach was successfully used to investigate the acceptability of TOT and HST models in papers [1] [2] [11] and [12]. In [3], a methodology to assess the reliability of the thermal model parameters estimated from measured data was presented.

Reference [4] introduces data quality control and data set screening techniques. Results show that model reliability can be increased by about 50% while decreasing model prediction error by applying data quality control and data set screening procedures.

Some sources of error that affect top-oil temperature prediction were discussed in [5]. Error source such as inadequate data gathering, inadequate model, improper discretization and bad data are investigated. And, it is found that some of the difference is due to the absence of driving variables in the model such as wind and rain.

1.4 Summary of Chapters

The rest chapters of this document are organized as follows. In Chapter 2, a detailed analysis of the existing models used in this project is presented. Chapter 3 discusses some factors that could affect the performance of transformer thermal models. Additional criteria used in determining the acceptability of the models are discussed in Chapter 4. In Chapter 5, a detailed introduction of the application and the Graphical User Interface design is provided. Chapter 6 focuses on the dynamic loading calculation. Some challenges of the algorithm design are also presented.

CHAPTER 2

SELECTED TRANSFORMER THERMAL MODELS

2.1 Introduction

The ultimate goal of this work is to produce a software-based application which can perform transformer dynamic loading calculations. To perform dynamic loading, a model of the transformer's thermal performance is needed in order to predict HST and TOT. A lot of research has been completed to evaluate and select the optimal thermal models for this software application [1]-[16]. While the IEEE Clause 7 models, [6], uses parameters calculated from transformer heat-run test report data, other more accurate models, [7]-[10], use coefficients distilled from measured data. In this section, a detailed review of the two models used in the software application and developed in this work is provided. The technique of linear regression, which is used in estimating the transformer model parameters from measured data, is discussed. The data format and some metrics for assessing reliability of models are also presented.

2.2 IEEE TOT Model (Top-Oil Rise Model)

IEEE loading guide Std. C57.91-1995 presents a model for predicting TOT. This top-oil-rise-over-ambient-temperature model (also called top-oil rise model), is a function of load and the load loss ratio [6]. This model is widely used by the electric-power industry in order to predict the TOT of substation distribution transformers. The parameters required to build the model are provided in the manufacturer's heat-run test reports.

The top-oil rise model is governed by a differential equation,

$$\tau_{oil} \frac{d\theta_o}{dt} = -\theta_o + \theta_u \quad (2.1)$$

whose solution is an exponential function:

$$\theta_o = (\theta_u - \theta_i)(1 - e^{-t/\tau_{oil}}) + \theta_i \quad (2.2)$$

$$\theta_u = \theta_{fl} \left(\frac{I_{pu}^2 \cdot R + 1}{R + 1} \right)^n \quad (2.3)$$

$$\tau_{oil,R} = \frac{C\theta_{fl}}{P_{fl}} \quad (2.4)$$

$$\tau_{oil} = \tau_{oil,R} \cdot \frac{\left(\frac{\theta_u}{\theta_{fl}} \right) - \left(\frac{\theta_i}{\theta_{fl}} \right)}{\left(\frac{\theta_u}{\theta_{fl}} \right)^{\frac{1}{n}} - \left(\frac{\theta_i}{\theta_{fl}} \right)^{\frac{1}{n}}} \quad (2.5)$$

$$I_{pu} = \frac{I}{I_{rated}} \quad (2.6)$$

where,

C : is the thermal capacity of transformer (Wh/°C)

I : is the load under consideration (kVA or A)

I_{rated} : is the rated load (kVA or A)

I_{pu} : is the ratio of specified load to rated load (per unit)

n : is an empirically derived exponent

R : is the ratio of load loss to no-load loss at rated load

t : is the duration of load (hours)

θ_{fl} : is the top-oil rise over ambient temperature at rated load (°C)

θ_i : is the initial top-oil rise over ambient temperature for $t=0$ (°C)

θ_o : is the top-oil rise over ambient temperature (°C)

θ_u : is the ultimate top-oil rise over ambient temperature rise (°C)

τ_{oil} : is the oil time constant for any load and for any specific top-oil temperature rise (hours)

$\tau_{oil,R}$: is the oil time constant at rated kVA (hours)

The variable θ_{fl} is obtained from off-line tests and corresponds to the full-load top-oil temperature rise over ambient. The exponent n approximately accounts for changes in load loss and oil viscosity caused by changes in temperature. Values for n used in these equations are shown in Table 2.1,

TABLE 2.1 VALUES OF THE EXPONENT n FOR DIFFERENT COOLING MODES

Type of cooling	n
OA	0.8
FA	0.9
Non-directed FOA	0.9
Directed FOA	1

where,

OA: is the oil-natural-air-natural cooling mode

FA: is the oil-natural-air-forced cooling mode

FOA: is the oil-forced-air-forced cooling mode

Equation (2.2) describes the transformer TOT rise over ambient behavior as a first order model. The TOT is given by

$$\theta_{oil} = \theta_o + \theta_{amb} = (\theta_u + \theta_i)(1 - e^{-t/\tau_{oil}}) + \theta_i + \theta_{amb} \quad (2.7)$$

where,

θ_{amb} : is the ambient temperature variation (°C)

θ_{oil} : is the top-oil temperature (°C)

For purposes of estimating transformer coefficients, a discretized version of (2.1) is formulated using the Backward Euler approximation for the time derivative given by

$$\frac{d\theta_o}{dt} \approx \frac{\theta_o[k] - \theta_o[k-1]}{\Delta t} \quad (2.8)$$

Substituting (2.8), (2.6) and (2.3) into (2.1), the discretized form of (2.1) is obtained

$$\theta_o[k] = \frac{\tau_{oil}}{\tau_{oil} + \Delta t} \theta_o[k-1] + \frac{\Delta t \cdot \theta_{fl}}{T_o + \Delta t} \left(\frac{(I_{pu}[k])^2 \cdot R + 1}{R + 1} \right)^n \quad (2.9)$$

where Δt is the sampling period and k is the time step index.

If $R > 1$ and $I_{pu}^2 R \gg 1$, an approximation of the TOT rise over ambient temperature can be written as follows:

$$\theta_o[k] = \frac{\tau_{oil}}{\tau_{oil} + \Delta t} \theta_o[k-1] + \frac{\Delta t \cdot \theta_{fl}}{\tau_{oil} + \Delta t} (I_{pu}[k])^{2n} \quad (2.10)$$

2.3 IEEE HST Model (Winding Hot-Spot Rise Model)

IEEE loading guide Standard C57.91-1995 provides a model for predicting HST rise over TOT [6]. This first-order model is described by the differential equation,

$$T_h \frac{d\theta_h}{dt} + \theta_h = \theta_{hu} \quad (2.11)$$

which has the solution,

$$\theta_h = (\theta_{hu} - \theta_{hi})(1 - e^{-t/T_h}) + \theta_{hi} \quad (2.12)$$

$$\theta_{hu} = \theta_{hr} \cdot I_{pu}^{2m} \quad (2.13)$$

where,

m : is an empirically derived exponent

t : is the time duration of load (min)

T_h : is the winding time constant at hottest-spot location (min)

θ_h : is the hottest-spot temperature rise over top-oil temperature (°C)

θ_{hi} : is the initial hottest-spot temperature rise over top-oil temperature (°C)

θ_{hr} : is the hottest-spot temperature rise over top-oil temperature at rated load (°C)

θ_{hu} : is the ultimate hottest-spot temperature rise over top-oil temperature (°C)

The suggested values of the exponent m used in temperature determination equations are given in Table 2.2.

TABLE 2.2 VALUES OF THE EXPONENT m FOR DIFFERENT COOLING MODES

Cooling Mode	m
OA	0.8
FA	0.8
Non-directed FOA	0.8
Directed FOA	1

The IEEE loading guide does not provide an explicit equation for calculating the winding time constant, T_h , but it indicates that the winding time constant may be estimated from the resistance cooling curve during thermal tests. The winding time constant is defined in [6] as the time it takes for the winding temperature rise over top oil temperature to reach 63.2% of the difference between final rise and initial rise during a load change. Because of the similarity of transformer designs and based upon SRP's suggestion, the default winding time constant is chosen to be 5.5 minutes for all the transformers in this software application.

Using the previous equations, the HST rise over TOT can be calculated and in return used to calculate the HST by using:

$$\theta_{hst}(t) = \theta_h + \theta_{oil}(t) = (\theta_{hu} - \theta_{hi})(1 - e^{-t/T_h}) + \theta_{hi} + \theta_{oil}(t) \quad (2.14)$$

where θ_{hst} is the hottest-spot temperature (°C)

In order to predict hottest-spot temperature, a discretized form of (2.11) is more convenient to use. The Backward Euler method is used to approximate the derivative term, which is given by,

$$\frac{d\theta_h}{dt} \approx \left(\frac{\theta_h[k] - \theta_h[k-1]}{\Delta t} \right) \quad (2.15)$$

Substituting (2.15) into (2.11) gives,

$$T_h \left(\frac{\theta_h[k] - \theta_h[k-1]}{\Delta t} \right) = \theta_{hu}[k] - \theta_h[k] \quad (2.16)$$

Substituting (2.6), and (2.13) into (2.16) and rearranging gives,

$$\theta_h[k] = \left(\frac{T_h}{\Delta t + T_h} \right) \theta_h[k-1] + \left(\frac{\Delta t}{\Delta t + T_h} \right) \theta_{hr} (I_{pu}[k])^{2m} \quad (2.17)$$

Typical values of parameters T_h and θ_{hr} are available in the transformer heat-run report.

2.4 ASU TOT Model (Top-Oil Model)

The top-oil rise model described in (2.1) is a simple model that captures the basic thermodynamics of the transformer load, while not properly taking into account the variation of ambient temperature. Thus, reference [7] suggests that a better first-order characterization of both loading and ambient temperature variations can be accomplished by appropriately including θ_{amb} into (2.1).

$$\tau_{oil} \frac{d\theta_{oil}}{dt} = -\theta_{oil} + \theta_u + \theta_{amb} \quad (2.18)$$

The solution of the new formulation is,

$$\theta_{oil} = (\theta_u + \theta_{amb} - \theta_{oil_i}) (1 - e^{-t/\tau_{oil}}) + \theta_{oil_i} \quad (2.19)$$

where θ_{oil_i} is the initial value of TOT at $t=0$.

Using the Backward Euler approximation, and substituting (2.3) into (2.18), results in (2.20):

$$\theta_{oil}[k] = \left(1 - \frac{\Delta t}{\tau_{oil} + \Delta t} \right) \theta_{oil}[k-1] + \frac{\Delta t}{\tau_{oil} + \Delta t} \theta_{amb}[k] + \frac{\Delta t}{\tau_{oil} + \Delta t} \theta_{fl} \left(\frac{I_{pu}^2[k] \cdot R + 1}{R + 1} \right)^n \quad (2.20)$$

For purposes of estimating transformer parameters from measure data, (2.20) can be formulated as follows:

$$\theta_{oil}[k] = (1 - K_2)\theta_{oil}[k-1] + K_2\theta_{amb}[k] + K_1I_{pu}^2[k] + K_3 \quad (2.21)$$

Noticed that (2.21) is a linear equation. Optimal $K_1 - K_3$ can be calculated from measured data using linear regression. This model was tested in [2] and [6]. The results indicated that the ASU TOT model does capture the dynamics associated with the ambient temperature, yielding a significant improvement over the IEEE model in the prediction accuracy.

2.5 ASU HST Model (Modified HST Model)

The IEEE HST model implies that all changes in HST rise over TOT are caused by changes in load. However, the effect of TOT variation on the HST rise over TOT is not considered. According to thermodynamic theory, HST will not change instantaneously even if TOT changes instantaneously. There is a time lag due to the winding time constant. The linearized HST model, also known as the ASU HST model, captures the effect of TOT variations on HST by changing the state variable in (2.11) from the HST rise (θ_h), to HST (θ_{hst}).

$$T_h \frac{d\theta_{hst}}{dt} + \theta_h = \theta_{hu} \quad (2.22)$$

where θ_h is defined as

$$\theta_h(t) = \theta_{hst} - \theta_{oil}(t) \quad (2.23)$$

Substituting (2.23) into (2.22) yields,

$$T_h \frac{d\theta_{hst}}{dt} + \theta_{hst} = \theta_{hu} + \theta_{oil}(t) \quad (2.24)$$

which has the solution,

$$\theta_{hst} = (\theta_{hu} + \theta_{oil}(t) - \theta_{hi}) (1 - e^{-t/T_h}) + \theta_{hsti} \quad (2.25)$$

where θ_{hsti} is the initial value of HST for $t=0$.

Using the Backward Euler approximation, equation (2.24) is discretized, resulting in (2.26):

$$T_h \left(\frac{\theta_h[k] - \theta_h[k-1]}{\Delta t} \right) = \theta_{hu}[k] + \theta_{oil}[k] - \theta_{hst}[k] \quad (2.26)$$

Substituting (2.6) in (2.26) and rearranging gives,

$$\begin{aligned} \theta_{hst}[k] &= L_{1m} \theta_{oil}[k] + (1 - L_{1m}) \theta_{hst}[k-1] + L_2 (I_{pu}[k])^{2m} \\ L_{1m} &= \left(\frac{\Delta t}{\Delta t + T_h} \right), L_2 = \left(\frac{\Delta t \cdot \theta_{hr}}{\Delta t + T_h} \right) \end{aligned} \quad (2.27)$$

The parameters of the ASU HST model, L_{1m} and L_2 , can be estimated from the measured data using linear regression.

2.6 Linear Regression and the Least-Squares Method

A multiple regression model that describes the relationship between the output response, y , and the k regressor (predictor) variables can be represented as follows:

$$y = \beta_0 + \beta_1 x_1 + \beta_2 x_2 + \dots + \beta_k x_k + \varepsilon \quad (2.28)$$

The parameters $\beta_j, j=0,1,\dots,k$ are called the regression coefficients. The model parameters are estimated by fitting the model to the measured data [17]. Suppose that $n > k$ observations are available, and let y_i denote the i^{th} observed response and x_{ij}

denote the i^{th} observation of the regressor, x_j . The error term, ε , is assumed to be normally distributed with mean zero and variance σ^2 , and the errors are assumed to be mutually uncorrelated. The least-squares method can be used to estimate the regression coefficients of equation (2.28). In matrix notation, (2.28) can be written as,

$$\mathbf{y} = \mathbf{X}\boldsymbol{\beta} + \boldsymbol{\varepsilon} \quad (2.29)$$

where \mathbf{y} is an $n \times 1$ vector of the observations, \mathbf{X} is an $n \times k$ matrix of the variables, $\boldsymbol{\beta}$ is a $k \times 1$ vector of the unknown regression coefficients and $\boldsymbol{\varepsilon}$ is an $n \times 1$ vector of random errors.

Thus, the least-squares estimator of $\boldsymbol{\beta}$ can be found by minimizing the function:

$$\mathcal{S}(\boldsymbol{\beta}) = \sum_{i=1}^n \varepsilon_i^2 = \boldsymbol{\varepsilon}^T \boldsymbol{\varepsilon} = (\mathbf{y} - \mathbf{X}\boldsymbol{\beta})^T (\mathbf{y} - \mathbf{X}\boldsymbol{\beta}) = \|\mathbf{y} - \mathbf{X}\boldsymbol{\beta}\|_2^2 \quad (2.30)$$

Expanding equation (2.30) results in:

$$\mathcal{S}(\boldsymbol{\beta}) = \mathbf{y}^T \mathbf{y} - 2\boldsymbol{\beta}^T \mathbf{X}^T \mathbf{y} + \boldsymbol{\beta}^T \mathbf{X}^T \mathbf{X} \boldsymbol{\beta} \quad (2.31)$$

The least-squares estimator must satisfy,

$$\frac{\partial \mathcal{S}(\boldsymbol{\beta})}{\partial \boldsymbol{\beta}} = -2\mathbf{X}^T \mathbf{y} + 2\mathbf{X}^T \mathbf{X} \hat{\boldsymbol{\beta}} = 0 \quad (2.32)$$

The least-squares estimator of $\boldsymbol{\beta}$, is given by

$$\hat{\boldsymbol{\beta}} = (\mathbf{X}^T \mathbf{X})^{-1} \mathbf{X}^T \mathbf{y} \quad (2.33)$$

The formulation presented in (2.29)-(2.33) can be used to estimate the transformer coefficients from measured data.

The top-oil model described in (2.21) can be rearranged as follows,

$$\theta_{oil}[k] - \theta_{oil}[k-1] = K_1 I_{pu}^2[k] + K_2 (\theta_{amb}[k] - \theta_{oil}[k-1]) + K_3 \quad (2.34)$$

Note that K_1 is proportional to the heat generated by the load in time Δt , K_2 is proportional to the heat lost to air during each time interval, and K_3 is proportional to heat generated by no-load losses. The objective function needed to find the coefficients that best minimize the cost function $S(\beta)$ is:

$$\hat{K} = \min_k \left\| \begin{bmatrix} (\theta_{oil}[k] - \theta_{oil}[k-1]) - [I_{pu}^2[k] \quad (\theta_{amb}[k] - \theta_{oil}[k-1]) \quad 1] \cdot \begin{bmatrix} K_1 \\ K_2 \\ K_3 \end{bmatrix} \end{bmatrix} \right\|_2^2 \quad (2.35)$$

Using (2.33) and the corresponding measured data the transformer coefficients K_1, K_2, K_3 can be estimated. A similar process is used to obtain the optimal parameters for the ASU HST model, L_{1m} and L_2 , from measure data, as shown below:

$$\hat{L} = \min_k \left\| \begin{bmatrix} (\theta_{hst}[k] - \theta_{hst}[k-1]) - [(\theta_{oil}[k] - \theta_{hst}[k-1]) \quad (I_{pu}[k])^{2m}] \cdot \begin{bmatrix} L_{1m} \\ L_2 \end{bmatrix} \end{bmatrix} \right\|_2^2 \quad (2.36)$$

2.7 Metrics for Model Reliability Assessment

After model building, there are two types of models for TOT/HST prediction: the IEEE models with parameters calculated from the transformer heat-run test report, and the ASU models with parameters obtained from measured data. If the measured input data are corrupted or insufficient to build a reliable ASU model, the application must be (and is) able to recognize it, and use the IEEE model as a backup.

In the existing application, several metrics are used to determine whether an ASU model is reliable and which model (IEEE model or ASU model) should be used.

2.7.1 Maximum Steady-State Load (SSL_{Max}) and Bootstrapping

An important metric that incorporates all transformer coefficients is steady-state load. Maximum steady-state load is the maximum load that can be sustained without violating TOT or HST operation limits when the load and ambient temperature remain constant. Under steady-state conditions, $\theta_{oil}[k+1] = \theta_{oil}[k]$. Using this constraint and then solving equation (2.34) for the load, gives the maximum steady-state load as follows:

$$SSL_{Max} = \sqrt{\frac{K_2(TOT_{max} - T_{amb}) - K_3}{K_1}} \quad (2.37)$$

where T_{amb} is the ambient temperature.

This assumes TOT is the limiting criterion. If HST is the limiting criterion, a similar result may be obtained:

$$SSL_{Max} = 2m \sqrt{\frac{L_{1m}(HST_{max} - TOT_{max})}{L_2}} \quad (2.38)$$

In this work, TOT_{max} is taken as 105 °C, HST_{max} is taken as 135 °C. The ambient temperature, T_{amb} , is taken as 117 °F, which is the typical worst-case condition SRP uses for calculating peak summer loading.

In order to load the transformer conservatively, a 95% conservative rating is selected (defined below), whose calculation requires bootstrapping. Bootstrapping is a statistical method that can make a smaller data set of size n “look” like a larger data set by taking multiple random samples, with replacement, of size n from the small data set. In this project, bootstrapping is used to form 3000 sets of samples. And then, for each data set, a

TOT and an HST model are built, yielding 3000 TOT/HST models. Each model is then used to predict maximum steady-state load. The process for this is shown in Fig. 2.1.

Because the data are always noisy, models built from different datasets will differ and produce different estimates of SSL_{Max} . In consultation with engineers from SRP, the 95% conservative rating of SSL_{Max} is used as the criteria of model selection. If the 95% conservative SSL_{Max} prediction is greater than 1.3 pu, the ASU model is treated as unreliable and will not be used.

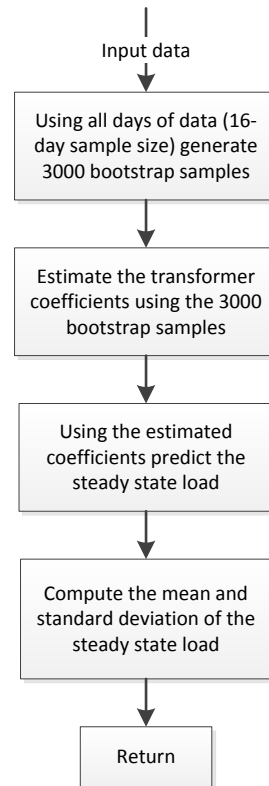


Fig. 2.1 Flowchart of bootstrapping

2.7.2 Variance Inflation Factors (VIF)

The covariance matrices of the estimated parameters $\boldsymbol{\beta}$ of a linear model is given as $\sigma^2(\mathbf{X}^T\mathbf{X})^{-1}$. The variable C_{jj} is the diagonal element of the matrix $(\mathbf{X}^T\mathbf{X})^{-1}$. The Variance Inflation Factor (VIF) for the j^{th} parameter is defined as:

$$VIF_j = C_{jj} \quad (2.39)$$

For a linear model, if the j^{th} parameter is orthogonal to or has little dependence on other predictor variables then C_{jj} is 1.0 or closes to 1.0. The VIF for each variable can be used as a metric that measures the combined effect of the dependencies among the variables on the variance of that term.

When the VIF of a variable is greater than 10, it means that the variable is highly dependent on other variables and the corresponding parameter is poorly estimated. Therefore, the model is unreliable.

2.7.3 Coefficient of Determination R^2

The coefficient of determination R^2 is defined as

$$R^2 = 1 - \frac{SS_{Res}}{SS_T} \quad (2.40)$$

where SS_T is a measure of total variation in the observations and SS_{Res} is the error sum of squares.

The R^2 value provides a measure of the variability explained by the model. A value closer to 1 is desired. In this work, models with $R^2 < 0.7$ are treated as unreliable.

2.8 Conclusions

The advantage of the IEEE models is that all the parameters need can be found in the heat-run test report. However, the IEEE models are criticized for their inaccuracy. The ASU models are linearized models which take into account the effect of ambient temperature. With parameters distilled form measured data by using linear regression, the ASU models are proved to have better performance in predicting TOT and HST. Several metrics are applied to assess model reliability and select the optimal model for dynamic loading calculation.

CHAPTER 3

IMPROVING MODEL PERFORMANCE

3.1 Introduction

In this research, it is found that the cooling fans in transformers sometimes do not turn on/off according to their specified set-points, or the set-points in the field are different from the values prescribed by the responsible engineers. Because thermal models can only make reliable predictions for one thermodynamic condition, the data used for model building must all come from transformer performance when all fans have the same status. Given that the measured data used in model building is separated into sets (i.e., cooling mode) based on the turn on/off set-points specified by engineering, if the set-points used for data parsing do not match those in the field, then data corresponding to more than one thermodynamic condition will be used to train the same model. Consequently, improper fan status could lead to poor quality models. In addition, the IEEE models are used for thermodynamic conditions where no ASU model is available. The performance of the IEEE models affects the calculated cooling mode transition points, and these erroneous transition points negatively impact the prediction results of the ASU models. A more detailed discussion of this complex issue is provided in the following subsections. Also, some researches to improve the model performance are presented in this chapter.

3.2 Cooling Modes

The transformer has a set of fans, and possibly pumps, which may be put in service to increase the power-carrying capacity at high loading. The cooling modes are defined by

the way cooling occurs: by natural convection or by a forced circulation system composed of fans or pumps.

For the light loading, the coolant circulation is by natural convection. The transformer is said to be in an oil-natural-air-natural cooling mode (ONAN or OA). The transformer that uses fans rather than pumps in service is in an oil-natural-air-forced cooling mode (ONAF or FA). Typically, when the first turn-on set-point is reached, only half of the fans turn on. At the second turn-on set-point, all fans come on and the mode is referred to as ONFAFA or more simply, FAFA, or FA/FA. If a transformer has oil pumps, then at the second turn-on set-point, both the fans and pumps are engaged, and the transformer is said to be in the oil-forced-air-forced cooling mode (OFAF or FOA) [18]. Data measured in the OA mode is classified as tier-1 data in this work. Data measured in the FA mode can be divided into two parts: when half the fans are on, which is classified as tier-2 data; and when all fans are on, which is classified as tier-3 data.

The on/off state of the fans and pumps is controlled by the HST. Historically, simulated HST was used to determine the cooling-modes transition points because HST was not measured directly. While measured HST is used in newer transformers, simulated HST is still used when measured HST is unavailable. Based on SRP's settings, the tier divisions typically occur as follows: tier-3 starts when HST (simulated or measured) exceeds 75 °C and ends when HST drops below 70 °C; tier-2 starts when HST rises over 65 °C and ends when the HST falls below 60 °C. The rest of the data is considered as tier-1 data, as shown in Fig. 3.1.

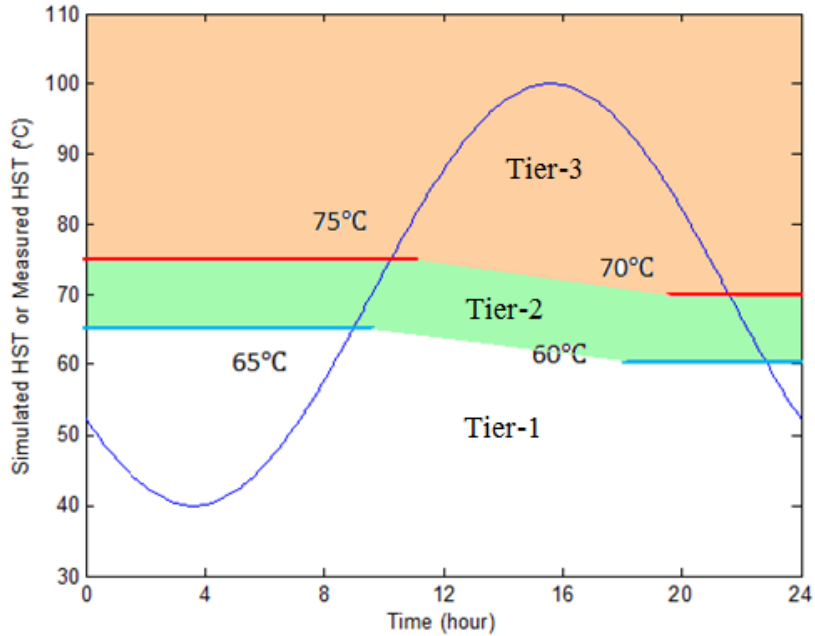


Fig. 3.1 Tier division

3.3 Improper fan status

The fan status of transformer DV10 is displayed in Fig. 3.2, which was provided by APS. The x-axis is the time of day and the y-axis is temperature in °C. In the figure, the yellow line is the TOT, the short red lines indicate the point in time when the fan turns on, and the short blue lines indicate the point in time when they turn off. The on/off state of the fans is controlled by the HST, according to their set-points. However, it may be observed in this figure that the turn-on-temperature and turn-off-temperature of the fans during different days is variable when it should be consistent. On the day 07/19, the fans turn on and then turn off immediately. On another day 07/27, the fans turn on and do not turn off, at least for the duration of the plot.

In this project, the measured data are separated into different tiers (cooling modes) according to the desired set-points provided to us by engineers at SRP. Since the ultimate application of this research is to predict transformer performance under over-loaded conditions (that is tier-3 cooling mode). The ASU models are created using only tier-3 data and are applied for tier-3 cooling mode prediction during the dynamic loading process. As stated earlier, inaccurate fan status could cause the ASU thermal models to be inaccurate by including data from more than one cooling mode.

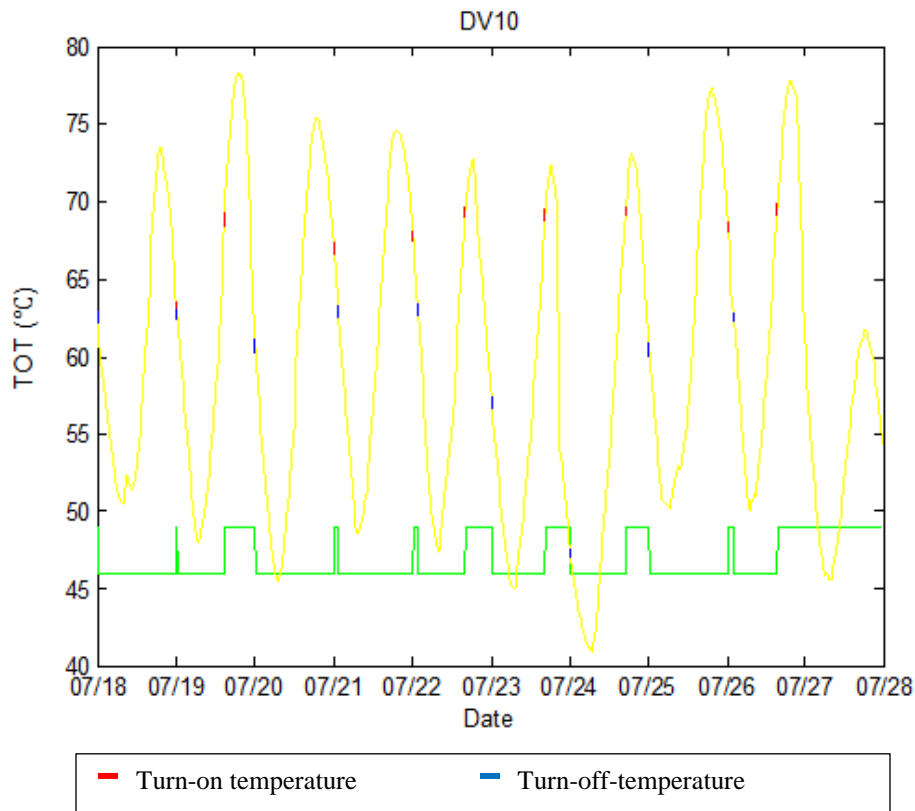


Fig. 3.2 Fan status of the transformer DV10

3.4 Bad Performance of the IEEE Models

The IEEE models are widely used in industry. However, the effects of ambient-temperature variation on TOT and HST are not properly taken into account and the prediction results of IEEE models are consequently inaccurate. The example below indicates how the poor performance of the IEEE models affects the accuracy of ASU models when used in temperature prediction.

Since the ASU model is only built for tier-3 operation, when predicting transformer temperature for a period in which tier-1 and tier-2 cooling occurs, the IEEE model must be used. In Fig. 3.3 the prediction results for TOT and HST are presented for a 24-hour period with the IEEE models used for predicting tier-1 and tier-2 performance and the ASU model used to predict tier-3 performance. For a comparison, the prediction results for TOT and HST with the TOT initialized to the measured value at tier-2-tier-3 boundary (to correct for the prediction errors caused by the IEEE model in tier-1 and tier-2 operation) is shown in Fig. 3.4. Observe that during tier-1 and tier-2 performance, the IEEE models predict both TOT and HST far below their measured value. The bad performance leading up to the tier-2-tier-3 boundary creates not only the wrong tier transition times but also a poor initial condition for the ASU tier-3 model (incorrect in Fig. 3.3 but corrected in Fig. 3.4), leading to obvious inaccuracies.

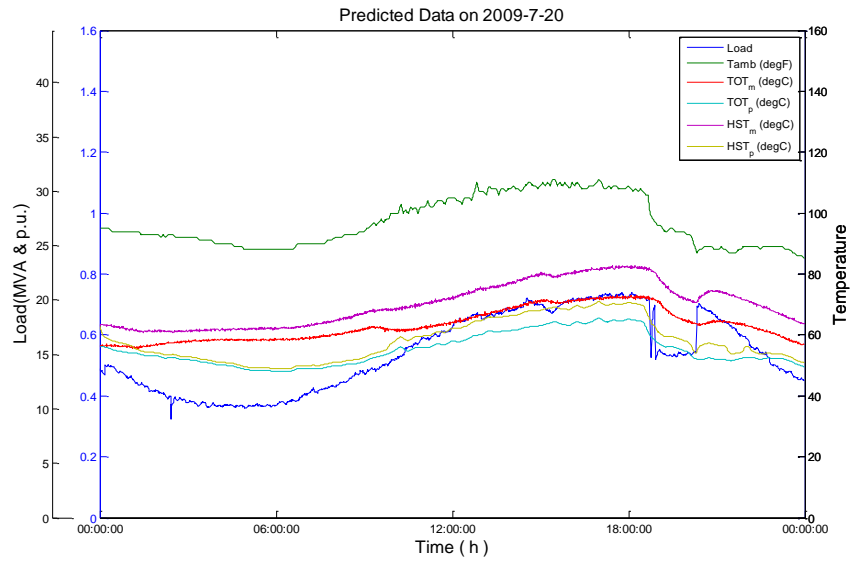


Fig. 3.3 Prediction results of Highline3 on 2009-7-20: tier-1 and tier-2 use IEEE models, tier-3 use ASU models

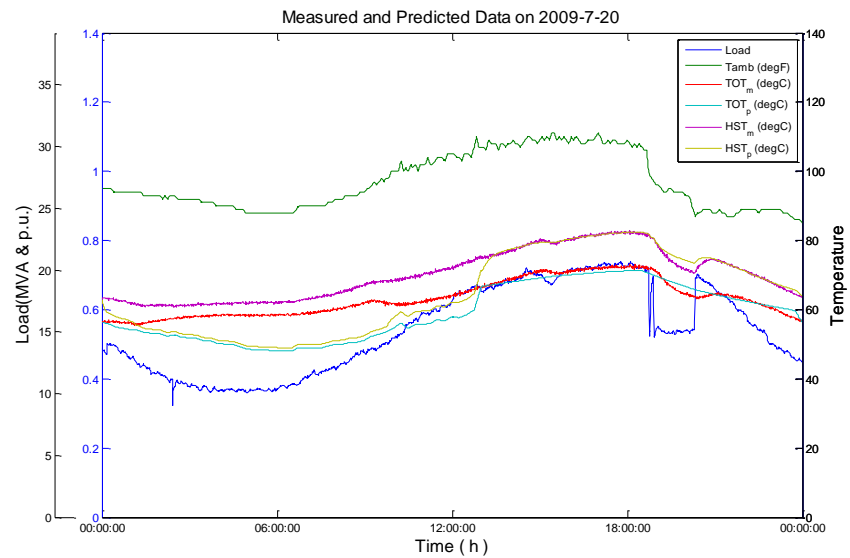


Fig. 3.4 Prediction results of Highline3 on 2009-7-20: tier-1 and tier-2 use IEEE models, tier3 use ASU models, with TOT alone initialized to the measured TOT value at tier-2-tier-3 boundary

3.5 Improving Model Performance

It was found that, some transformers have cooling mode set-points that do not follow the rules mentioned above. Instead of the transition point vector shown in Fig. 3.1, i.e., (65, 75, 70, 60)°C, these transformers use (75, 75, 60, 60)°C for cooling mode transition set-points, which means there are only two cooling modes for those transformers. The results of building ASU models using the data consistent with both transition point vectors are displayed below:

TABLE 3.1 ESTIMATED MODEL PARAMETERS BASED ON COOLING MODE SET-POINT VECTOR (75, 75, 60, 60)°C

Transformer Name	K_1	K_2	K_3	K_4	Time Constant (hr)	SSL_max (pu)	RMS Error
Highline3	1.3597	0.0899	0.9100	1.9423	2.5292	1.5825	2.5542
Kirk2	1.1732	0.0870	0.9130	1.8107	2.6228	1.6928	2.2610
Moody1	3.4832	0.1277	0.8723	1.8076	1.7073	1.2887	0.7758
Pendergast2	2.6255	0.1252	0.8748	2.1018	1.7472	1.4261	1.4233
University2	1.8237	0.0772	0.9228	1.9151	2.9866	1.2115	1.1954

TABLE 3.2 ESTIMATED MODEL PARAMETERS BASED ON COOLING MODE SET-POINT VECTOR (65, 75, 70, 60)°C

Transformer Name	K_1	K_2	K_3	K_4	Time Constant (hr)	SSL_max (pu)	RMS Error
Highline3	3.8543	0.1261	0.8739	1.9264	1.7322	1.2022	1.2080
Kirk2	1.9674	0.1081	0.8919	2.0437	2.0626	1.4925	1.5591
Moody1	3.6669	0.1249	0.8751	1.5959	1.7511	1.2610	0.5723
Pendergast2	3.3483	0.1388	0.8612	2.0992	1.5515	1.3553	0.7213
University2	2.1997	0.0917	0.9083	2.2374	2.4749	1.2092	0.6099

Table 3.1 gives the estimated model parameters based on cooling mode set-point vector (75, 75, 60, 60)°C, and Table 3.2 is for the model parameters with transition point vector (65, 75, 70, 60)°C. By comparing these two tables, it is found that both time constants and SSL_{\max} decrease when the three-cooling-mode model is assumed. And, there is a significant improvement on the root-mean-square (RMS) error. When using the cooling mode set-points (75, 75, 60, 60) °C, all the data are divided into on two tiers, tier-1 or tier-3, in this program. From these results it appears that the tier-data parsing using (75, 75, 60, 60) °C is incorrect, which leads to part of the tier-2 data being used to build tier-3 models, making the ASU models inaccurate.

3.6 Results of Model Performance

3.6.1 Highline3 Transformer

Fig. 3.5 shows the TOT prediction for the five hottest days during the period 2-8 PM based on different cooling mode set-points. The measured TOT (red line), the TOT predicted by the ASU model (dotted-dashed blue line) and the TOT predicted by the IEEE model (dashed purple line) are displayed in the figure for comparison. Comparing (a) and (b) in Fig. 3.5, it is found that the ASU model built with transition point vector (65, 75, 70, 60) °C predicts TOT more accurately. Fig. 3.6 shows the TOT and HST prediction results on 2009-7-27 for those two cooling mode transition point vectors.

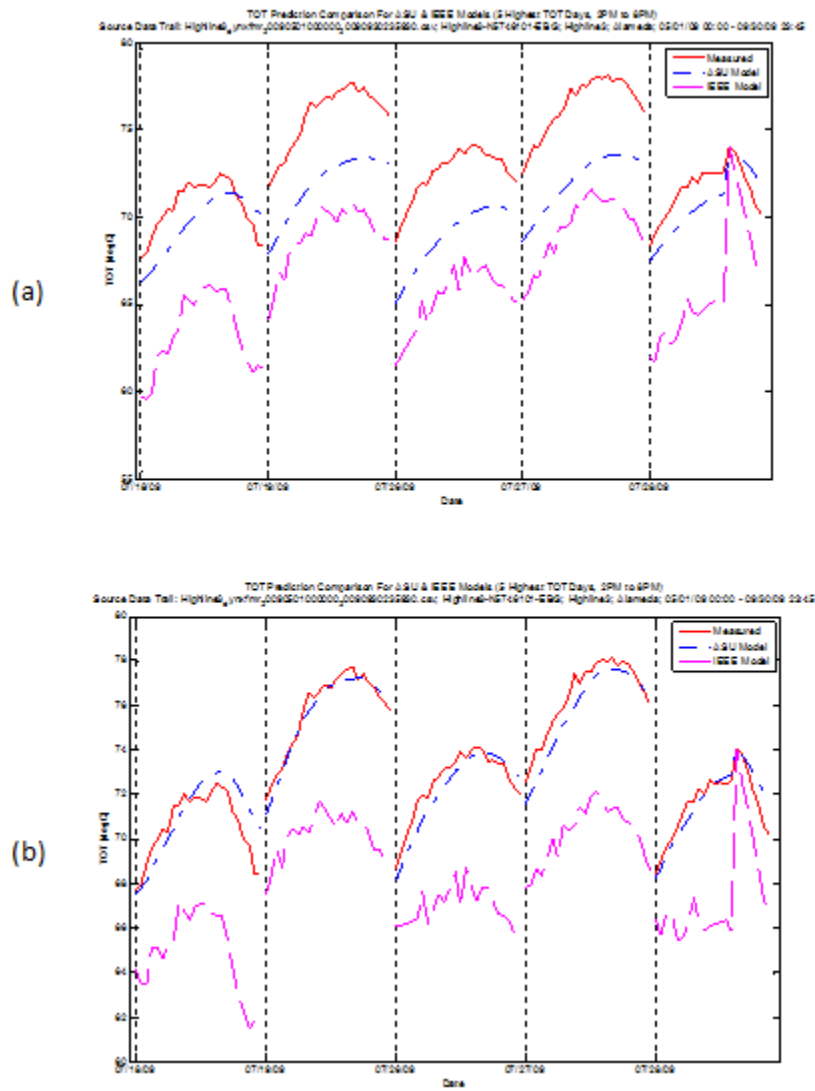


Fig. 3.5 TOT prediction for 5 hottest days for transformer Highline3: (a) cooling mode set-point vector (75, 75, 60, 60) °C; (b) cooling mode set-point vector (65, 75, 70, 60) °C

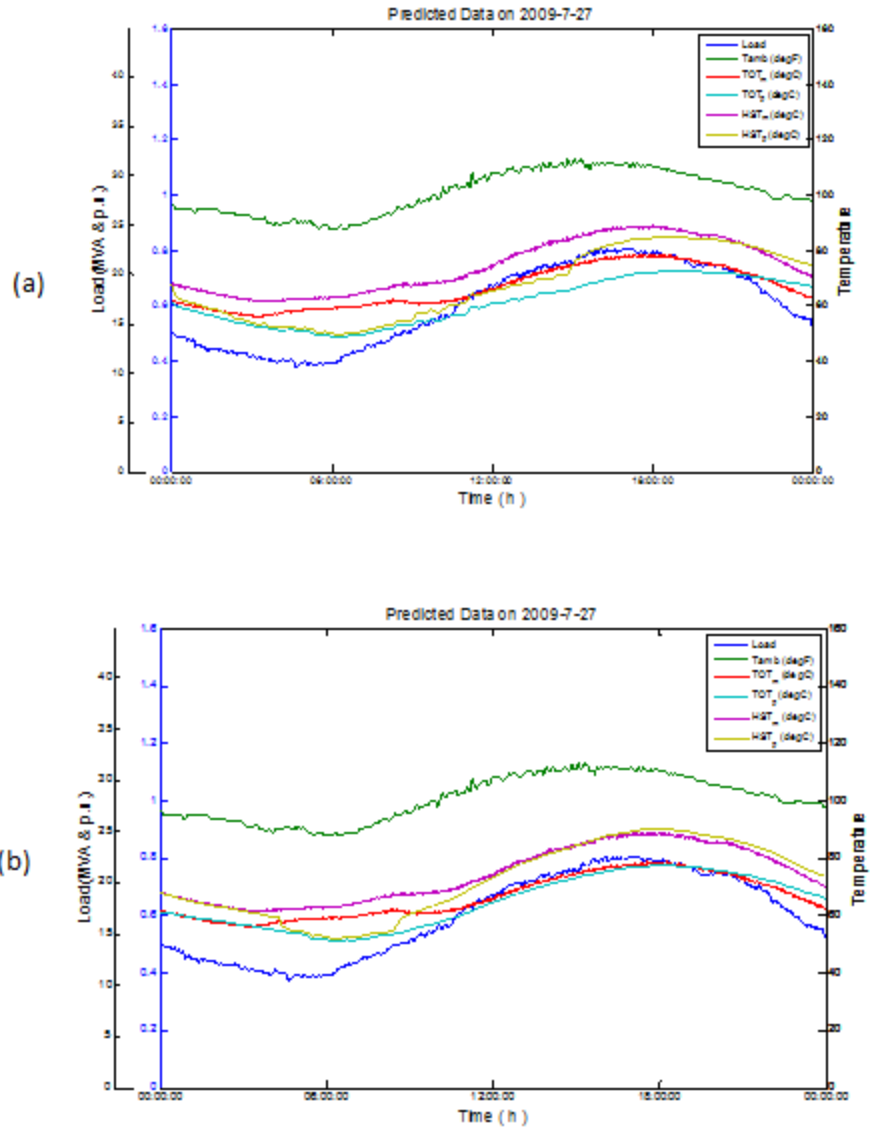


Fig. 3.6 Predicted TOT and HST on 2009-7-27 for transformer Highline3: (a) cooling mode set-points (75, 75, 60, 60) °C; (b) cooling mode set-points (65, 75, 70, 60) °C

3.6.2 Kirk2 Transformer

Fig. 3.7 shows the TOT prediction for the five hottest days during the period 2-8 PM based on different cooling mode set-points. The measured TOT is displayed using a red line, the TOT predicted by the ASU model is displayed using the dotted-dashed blue line,

and the TOT predicted by the IEEE model is represented using the dashed purple line. Compare (a) and (b) in Fig. 3.7, it is found that the ASU model built with cooling mode set-points (65, 75, 70, 60) °C has better performance in matching the measured data. Fig. 3.8 shows the TOT and HST prediction results on 2009-7-17 for those two sets of cooling mode set-points.

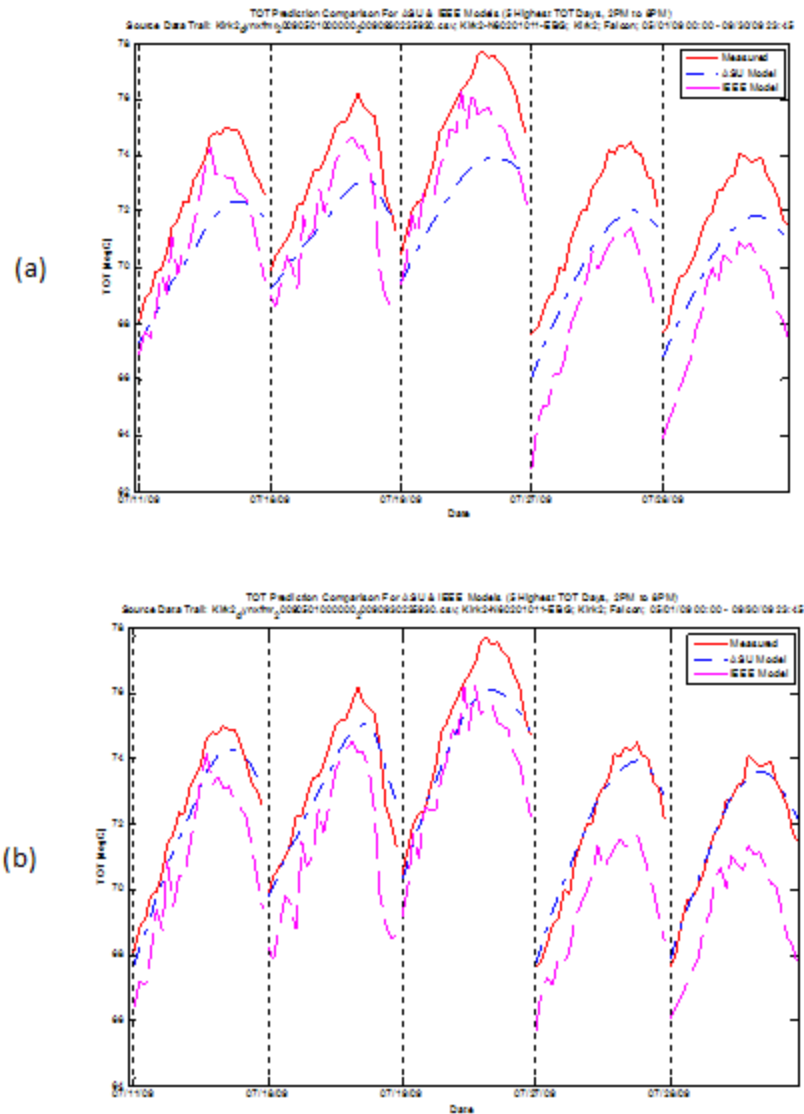


Fig. 3.7 TOT prediction for 5 hottest days for transformer Kirk2: (a) cooling mode set-points (75, 75, 60, 60) °C; (b) cooling mode set-points (65, 75, 70, 60) °C

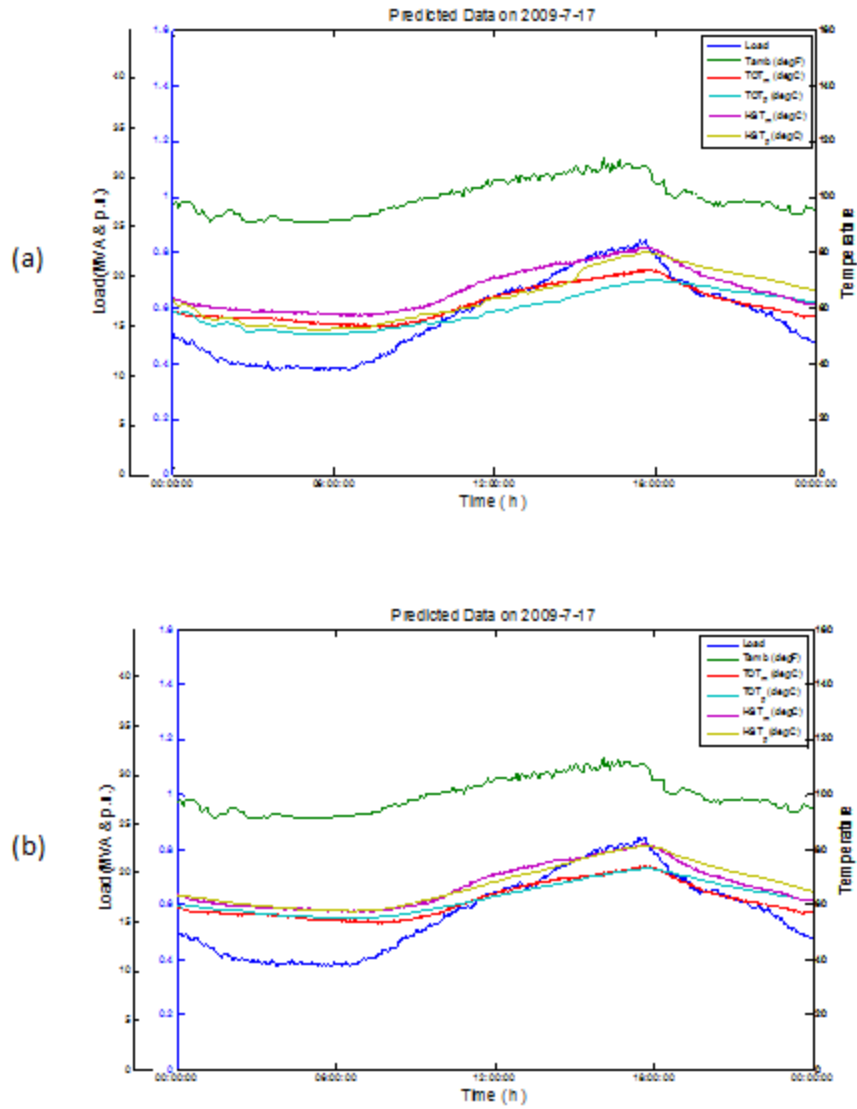


Fig. 3.8 Predicted Data on 2009-7-17 for transformer Kirk2: (a) cooling mode set-points (75, 75, 60, 60)°C; (b) cooling mode set-points (65, 75, 70, 60)°C

3.7 Conclusions

Both improper fan status and the IEEE models' poor performance could impact the prediction results of the ASU models, because of the erroneous cooling mode transition points. For some transformers, changing the cooling mode set-points can improve their models' performance.

CHAPTER 4

ADDITIONAL CRITERIA FOR MODEL SELECTION

4.1 Introduction

Before the improvements reported here were added to the existing application, several metrics (mentioned earlier) were applied to determine whether an ASU model was reliable and which model (IEEE model or ASU model) should be used. These metrics are:

- Maximum Steady-State Load (SSL_{Max})
- Variance Inflation Factors (VIF)
- Coefficient of Determination (R^2)

However, it was found that more consistent “good model” determination could be obtained if additional metrics were used. Additional criteria used in determining the acceptability of the ASU models are introduced and defined in this chapter. These criteria are applied to evaluate the acceptability of the ASU models in this chapter.

4.2 Model Testing on Webber3

To evaluate the model’s prediction performance, validation under interpolation and extrapolation should be verified. Interpolation performance is measured based on predicted values inside and on the boundary of the given data. The accuracy of predicted values significantly outside the range of given (training) data set is a measure of extrapolation performance. Since this application is to predict the maximum dynamic loading, which is an overloaded condition, the extrapolation performance of the model is important.

From all the data provided by SRP, only transformer Webber3 is found to have two overloaded days (8/20/2009 and 8/21/2009) with a step load change in the load curve, thus, Webber3 is selected for testing the model's extrapolation performance.. To conduct this testing, the ASU models are built (trained) on historical data under normal load conditions (excluding the two aforementioned overloaded days), then the models were used, together with the load profile and ambient temperature profile, to predict TOT and HST for the two overloaded days..

Here, two cases are considered:

Case 1: For tier 1 and tier 2, use IEEE model; for tier 3, use ASU model.

Case 2: For tier 1 and tier 2, use IEEE model; for tier 3, use ASU model with the TOT alone initialized to the measured TOT value at tier 2-3 boundary.

The results are shown as follows:

4.2.1 Simulation Results for 8/20/2009:

Fig. 4.1 corresponds to case 1 and Fig. 4.2 corresponds to case 2. Observe that the ASU models under-predict both the TOT and HST, which means the ASU models will over predict the amount of load that can be added per dynamic loading calculation. By comparing Fig. 4.1 and Fig. 4.2, it is found that most of the error in the TOT and HST prediction is due to the poor initial starting point of the tier-3 simulation, which is the end point of the IEEE model tier-2 simulation. When the starting point of tier-3 simulation is corrected to the measured value, as opposed to the tier-2 simulated value, as shown in Fig. 4.2, the error at the peak point in both TOT and HST for the ASU models are reduced to from 10.43 °C and 9.23 °C to 5.68 °C and 4.39 °C, respectively.

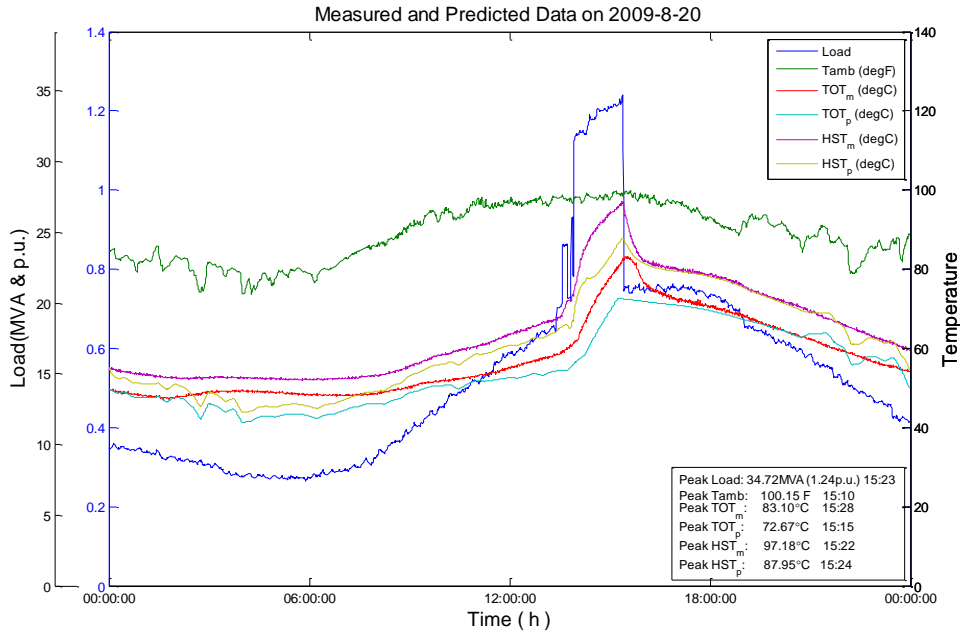


Fig. 4.1 Measured and predicted data for 2009-8-20 (case 1)

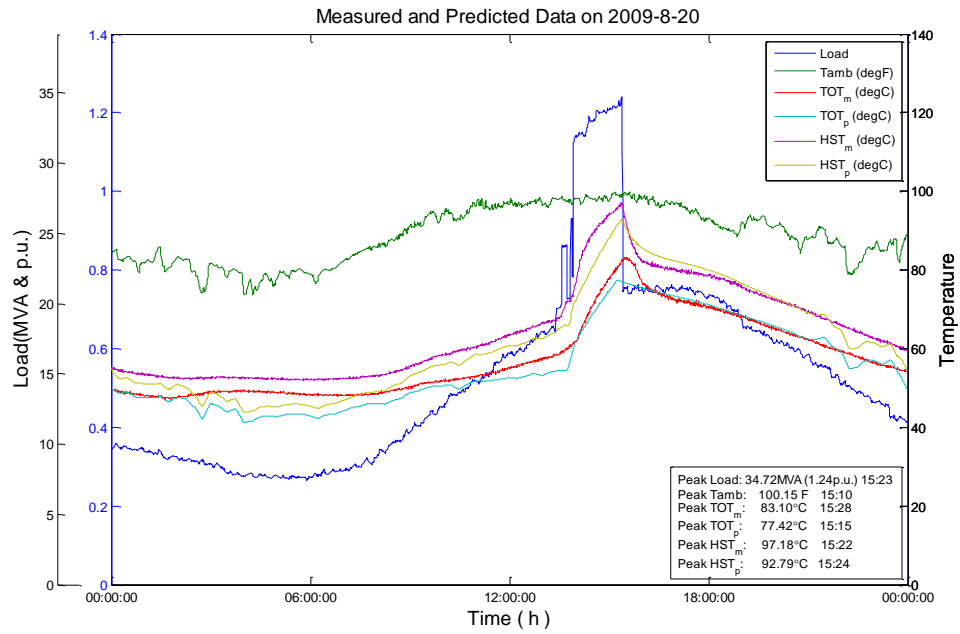


Fig. 4.2 Measured and predicted data for 2009-8-20 (case 2)

4.2.2 Simulation Results for 8/20/2009

Fig. 4.3 corresponds to case 1 and Fig. 4.4 corresponds to case 2. Observe that, the ASU models over-predict the TOT and HST by 0.32°C and 4.5°C respectively. When initializing the starting point of the tier-3 simulation to the measured value, as shown in Fig. 4.4, the error at peak point of the predicted TOT and HST curves increases by 1.46 °C and 2.29 °C respectively.

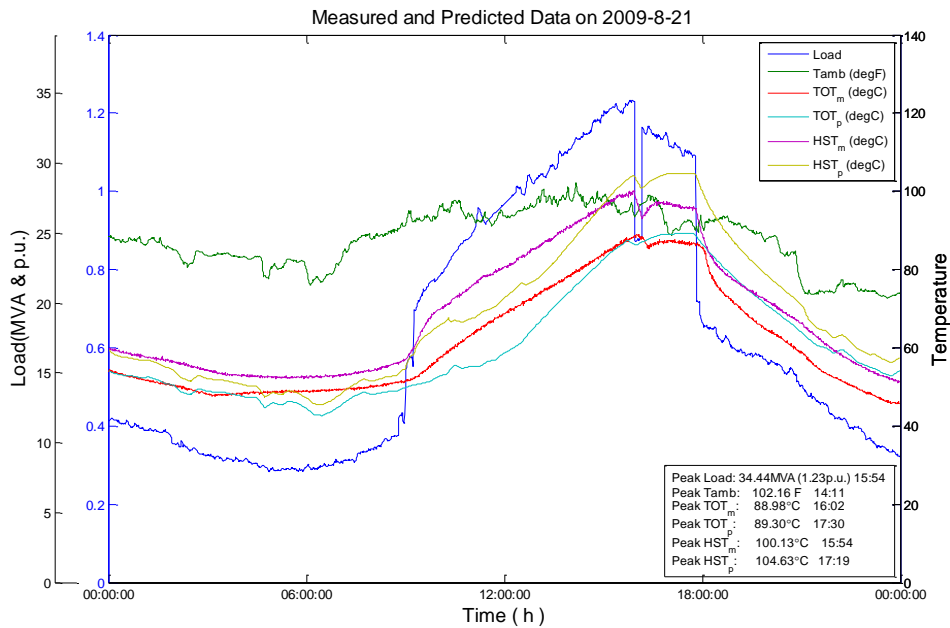


Fig. 4.3 Measured and predicted data on 2009-8-21 (case 1)

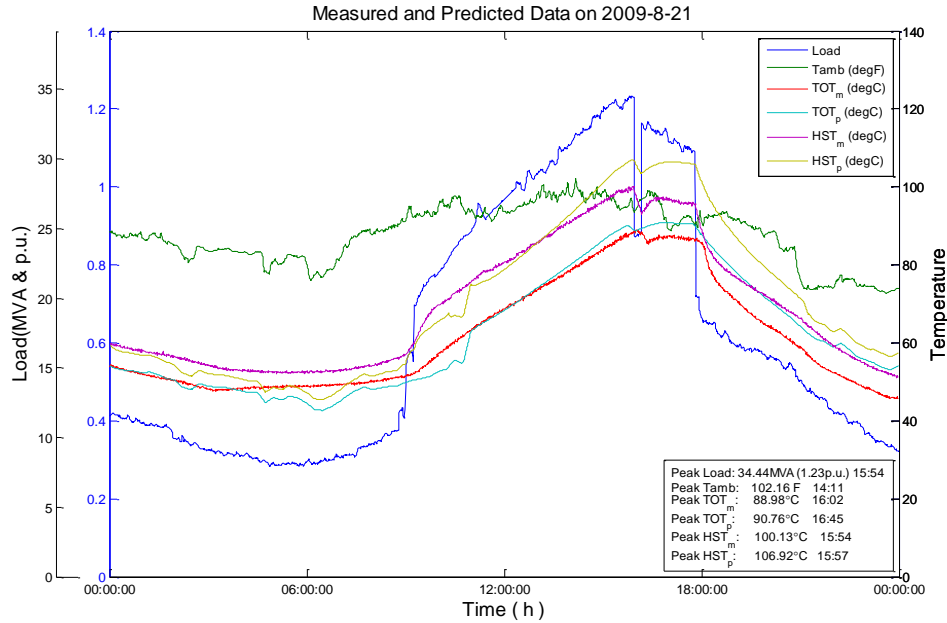


Fig. 4.4 Measured and predicted data on 2009-8-21 (case 2)

4.2.3 Overall conclusion:

The IEEE models used to predict tier 1 and tier 2 performance lead to errors that are carried forward into the tier 3 predictions, adding to the inaccuracy to the prediction of a transformer's thermal performance.

To some degree, the error in the TOT model contributes to increased error in the HST prediction because the HST prediction is based on the TOT prediction.

Both days (8/20/2009 and 8/21/2009) studied for Webber-3, the only transformer for which we have significant overloads, have similar ambient temperature curves, but have different load shapes. It is seen that the ASU models give different qualitative performances on these two days: it under-predicts for 2009-8-20 and over-predicts for 2009-8-21. Why this difference occurs is a subject of ongoing research.

4.3 Additional Metrics for Model Selection

Clearly, the values of the model parameters affect the performance of the model. From an engineering point of view, these parameters may be massaged to produce two metrics which are intuitively meaningful and whose effect on the simulations can be seen: the SSL_{max} and the top-oil time constant. If either the time constant or the steady-state load is too large or too small the model predictions will be inaccurate. As introduced in Chapter 2, the maximum steady-state load (SSL_{max}) has already been chosen to be a criterion of model reliability evaluation. In the following section, the time constant will be introduced as an additional criterion for model selection.

4.3.1 Time Constant

One type of metric that is often used for screening models derived from measured data is the so-called guide parameter. Guide parameters are physical model parameters for which either the values are approximately known or the bounds are known. The guide parameter chosen for model screening in this work is the top-oil time constant, rather than the HST time constant for the following reasons. It is known that the HST time constant is about 5-7 minutes. The value is so small, compared to the TOT time constant (about 2.5 hours,) that in some calculations it is ignored and the HST response is taken as instantaneous. Further, since the HST prediction is based on TOT prediction, the TOT time constant is ultimately more critical to model accuracy. Thus, only the ASU TOT model time constant was selected and is studied below.

As mentioned in Chapter 2, the parameters K_1, K_2 and K_3 can be estimated from measured data using linear regression. From equation (2.20) and (2.21), the time constant can be derived as follows:

$$K_2 = \frac{\Delta t}{\Delta t + \tau_{oil}} \quad (4.1)$$

$$\tau_{oil} = \frac{\Delta t}{K_2} - \Delta t \quad (4.2)$$

where the sampling period Δt is 0.25 hour (15 minutes) for the TOT model.

The time constants for the 15 transformers listed in Table 4.1 were calculated from the ASU tier-3 model coefficients distilled from measured data. A scatter chart of all of these time constants, which is shown in Fig 4.1, gives a different view of this data.

TABLE 4.1 TIME CONSTANT FOR 15 TRANSFORMERS

Transformer Name	Time Constant (hour)	Transformer Name	Time Constant (hour)
Broadway4(09)	4.19	Moody1(09)	1.71
Broadway4(10)	4.61	Moody1(10)	1.83
Cheatham2(09)	1.52	Pendergast2(09)	1.75
Cheatham2(10)	1.74	QueenCreek3(10)	1.82
CitrusHeights0(09)	1.55	QueenCreek4(09)	1.89
CitrusHeights0(10)	1.54	Sage4(09)	3.10
Clark2(09)	1.87	Sage4(10)	3.08
Clark2(10)	2.21	Tryon2(09)	1.68
Egan2(09)	1.77	Tryon2(10)	2.35
Highline3(09)	2.53	University2(09)	2.99
Highline3(10)	2.01	University2(10)	4.70
Kirk2(09)	2.62	Webber3(09)	2.43
Kirk2(10)	1.96	Webber3(10)	2.87

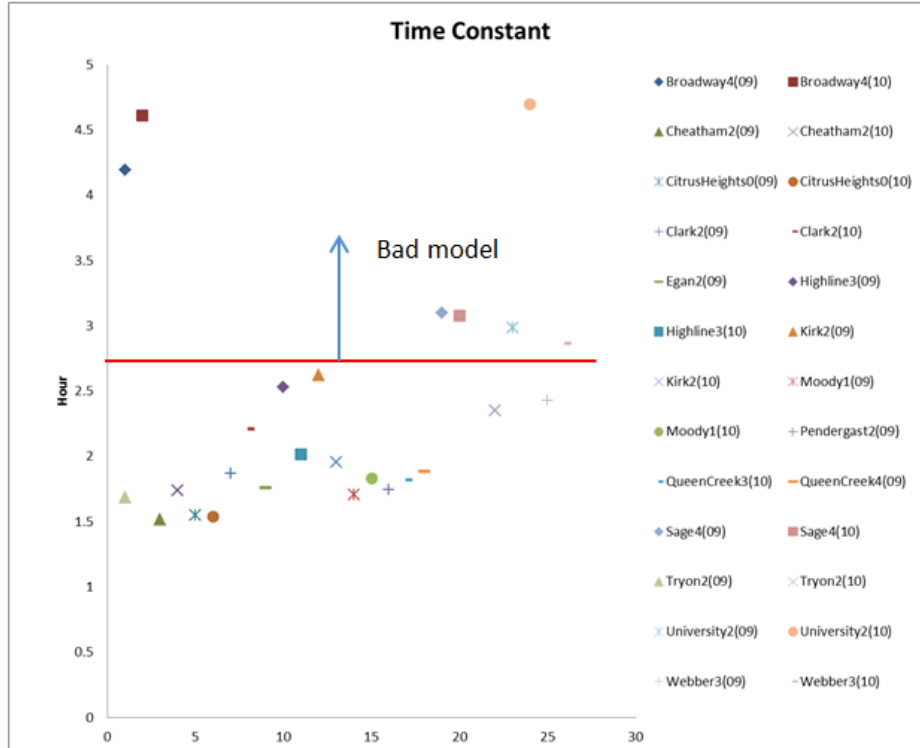


Fig. 4.5 Time constant for 15 transformers

In this research, when the time constant is larger than 2.75 hours, it was observed that the model prediction performance was poor. Thus, $\tau_{oil} < 2.75$ hours is used as a criterion of model selection.

4.3.2 Other Criterion for Model Screening

Another criterion being used for model screening is the ASU TOT model parameter K_3 , which is proportional to heat generated by no-load losses. K_3 should be larger than 0. Thus, models with $K_3 < 0$ are regarded as bad models and are not be used by the application developed.

4.4 Conclusion

Results show that additional metrics, such as the time constant and the model parameter K_3 , are needed to evaluate the acceptability of the ASU models.

CHAPTER 5

THE APPLICATION AND GUI DESIGN

5.1 Introduction

During peak summer loading, when an outage occurs, it is necessary to perform switching action on feeders so that customer load is picked up by transformers adjacent to the one out of service. This process is done today in a rather cumbersome way. When a substation distribution transformer overloading alarm is sent to the dispatcher, the dispatcher will determine which breakers to open and which to close in order to switch the load between transformers. Since estimating the overloading capability of a substation distribution transformer is complicated, the amount of load that is switched on or off is usually determined by taking a guess based on the experience of dispatchers or by consulting with planning engineers.

Over several years and under guidance of the SRP engineers, a planning tool, TTeMP, has been developed to build transformer thermal models that allow planning engineers to predict peak loads. The process for building these models requires several steps, some of which are quite lengthy, for example gathering and formatting measure data. This application calculates peak loading capability assuming a given load shape that was usually taken from historical data. This application was inappropriate for use by load specialists in a real-time environment for two main reasons. First, dispatchers do not have the time to perform the steps needed for model building; second the load shape for which they want to calculate maximum loading will not be based solely on historical data, but will have load step changes reflective of discrete switching on/off of load.

During the last two years, great stride has been made in developing a dynamic loading application for the dispatchers and load specialists. This Dynamic Loading of Transformer Application (DLTA) is created by using the existing planning application TTeMP as a starting point.

In this chapter, a detailed introduction of this DLTA application and Graphical User Interface design will be provided.

5.2 The Program Design

Since there has been no way to easily estimate the real-time loading limit, an off-line calculation incorporating the previous day's loading and temperature profiles as well as specific transformer parameters is used to determine the dynamic loading capability which lies within an acceptable confidence interval. Automation of this calculation and making it available as a real-time tool for the dispatchers and load specialists is the goal of this work. And, also, try to make it as easy and simple as possible.

5.2.1 Function Design

Salient functional specifications of this application include:

- a. Read and process data
 - i. Read historical data file
 - ii. Read real-time data file
 - iii. Read typical data file
 - iv. Read transformer model parameter data file
- b. Get user input and check input
- c. Search for the most "similar day"

- d. Perform dynamic loading calculation
 - i. Maximum load estimation
 - ii. Maximum duration estimation
- e. Output results

In this application, two scenarios are considered for the dynamic loading calculation:

Fixed-duration maximum-step-load increment calculation: If the user specifies the duration and the start time of the load increment, the program will compute the maximum step-load increment that the transformer can sustain without violating the TOT and HST thermal limits.

Fixed-load-increment maximum-duration calculation: If the user specifies the step-load increment and the start time of the load increment, the program will compute the maximum duration that the load change can be sustained without violating the TOT and HST thermal limits by the transformer.

5.2.2 Directory Structure and Data Files

Each folder and file in Fig. 5.1 is explained below:

- “DLTA”: the root directory for the application which contains other folders and files.
- “Execution Module”: the executable file for the application
- “Data”: this folder is the root directory for all the data files.
- “TOT&HST_data”: this folder contains data files which contain the measured TOT, HST, load and ambient temperature data.
- “Typical_data”: a folder contains typical load shape and ambient temperature data

files for use when no corresponding historical data is available.

- “RealTime_data”: this folder contains real-time data files which contain measured TOT, HST, load and ambient temperature data.
- “XfmrModelParameters”: this is a .csv file that contains IEEE and ASU model parameters of all the transformers.

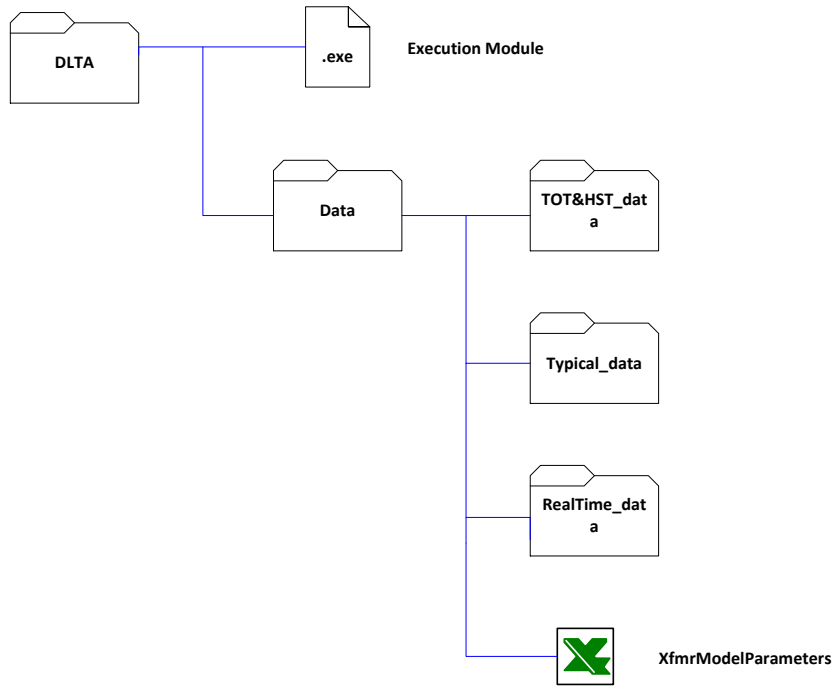


Fig. 5.1 Directory structure of the DLTA

5.2.3 Flowchart

The overall flowchart of the program is shown in Fig. 5.2. The first module is to set up search path to the installation directory

1. The first module is to set up search path to the installation directory.
2. Then, read in transformer model parameter (.csv) file and create a data structure.

3. From point A to point B is a loop to select a transformer for dynamic loading calculation, and to check whether the model information of the selected transformer is valid.
4. From point B to point C is to get the user input and check whether the input is valid.
5. From point C to the end is to select a type of data (“Historical data” or “Typical data”) for dynamic loading calculation
6. Finally, display the results.

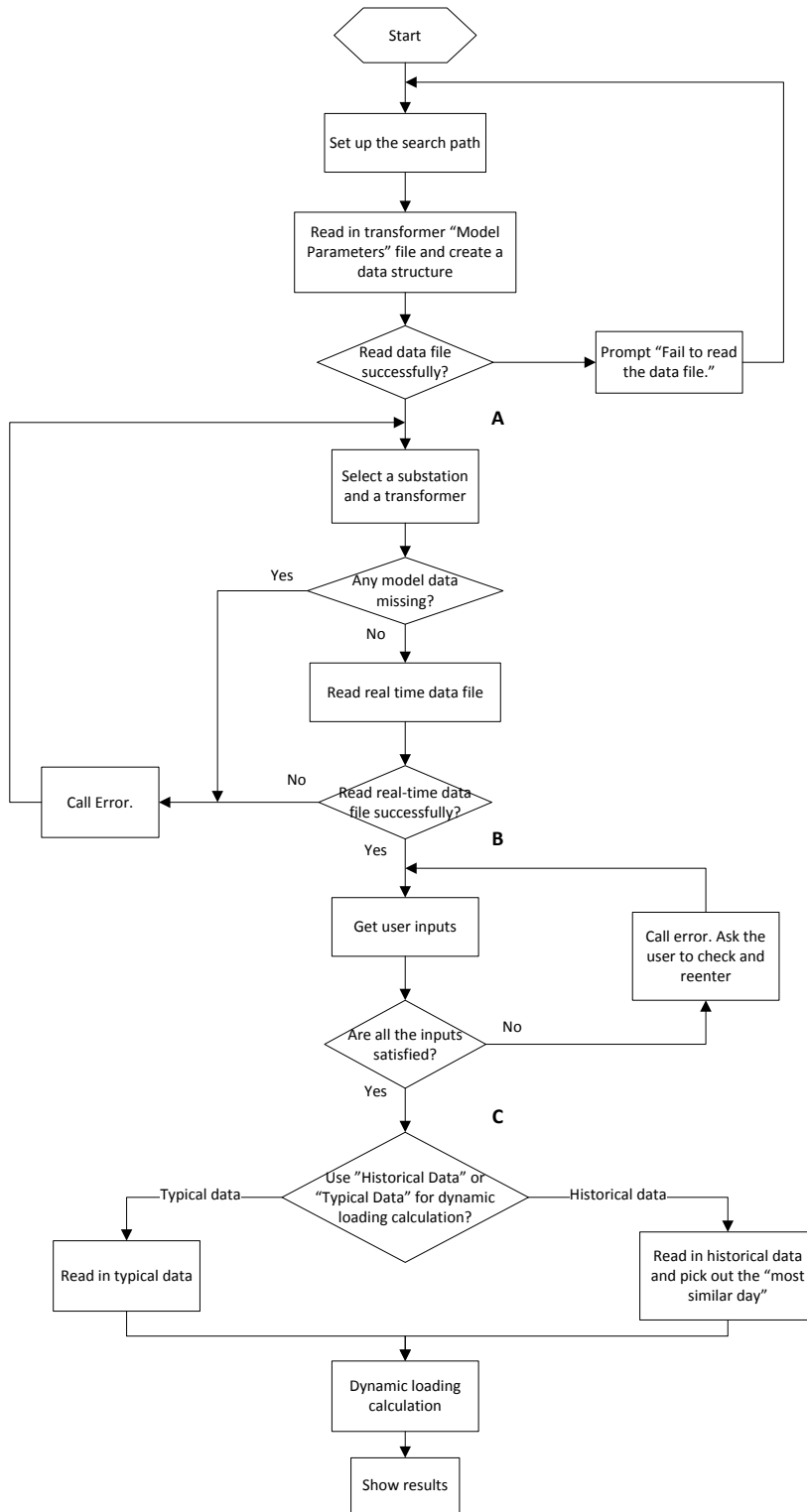


Fig. 5.2 The overall flowchart of the program

5.3 GUI Design

5.3.1 Startup Interface

Once the installation of the DLTA application is complete (see the user's manual) the next step is to start DLTA. Contained in Fig. 5.3 is a screenshot of the startup interface of the application. The user needs to input or browse to designate the path to DLTA's root directory before starting the application. After the search path is specified, the application will access the data folder, and read in transformer model coefficients which are stored in the file "Model Parameters.csv" to build a transformer data file for later use. A progress bar is displayed to show the progress of the data reading process. After this data is read in, the program will enter the main window and the startup interface will disappear and be concealed.

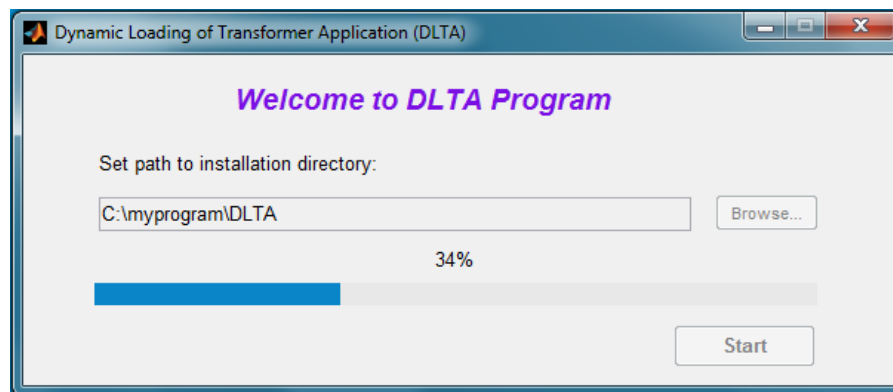


Fig. 5.3 Startup Interface

5.3.2 Main User Interface and Functional Area

Contained in Fig. 5.4 is a screenshot of the user interface. This interface can be divided into two functional areas: input area and output area. The GUI functional areas are discussed separately in the coming sections.

Select a substation: Broadway

Select a transformer: Broadway4-N60201010...

Enter MVA increment: 23 MVA (Should be less than 42 MVA)

Enter enhanced load duration: Hours

Select start time of load increment: 11 : 30

Enter high and low forecast temperatures: Min 70 Max 107 F
Low >15 degF High < 125 degF

	IEEE Model	ASU Model
Duration:	0 d 3 h 40 min	0 d 4 h 15 min
Load increment:	23 MVA	23 MVA

Dynamic Loading Calc

Fig. 5.4 Main User interface

5.3.3 Input Area

In order to perform dynamic loading calculation, some information must be entered as follows:

- Select a substation and a specific transformer
- Enter either MVA increment or enhanced load duration
- Enter the start time of load increment
- Enter the highest and lowest forecast ambient temperatures
- Click on “Start” button to perform dynamic loading

5.3.3.1 Select a Substation and a Transformer

All the transformers are classified by the substation to which they belong. As shown in Fig. 5.4, drop-down boxes are used in the substation and transformer selection. Each initiates the appearance of a drop-down box. Clicking on the drop-down arrow to the right of “Select a substation”, displayed in Fig. 5.5, allows the user to select an appropriate name from the drop-down list.

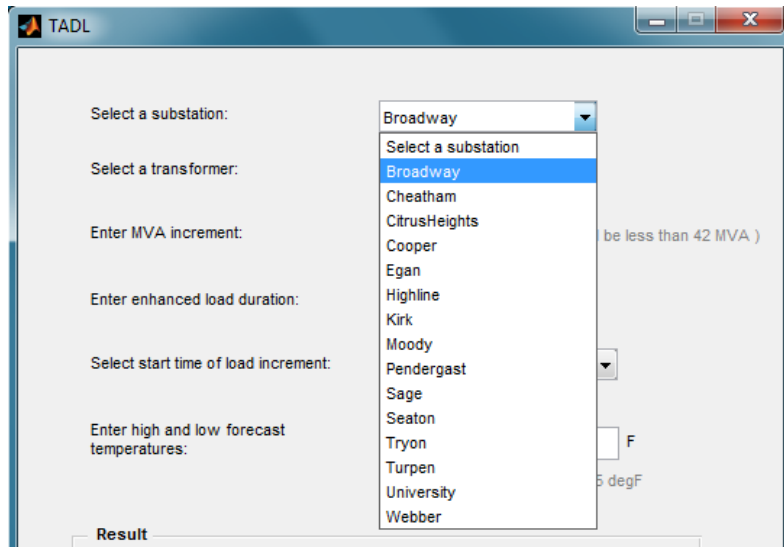


Fig. 5.5 Select a substation

After the substation is specified, all the transformer names associated with that substation are displayed in the second drop-down box, as shown in Fig. 5.6. From this drop-down box, the user selects the transformer name.

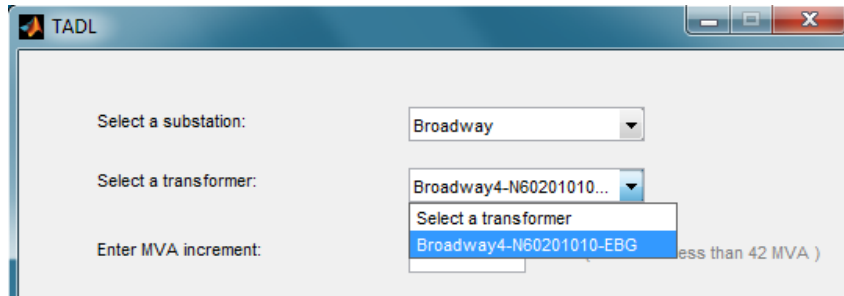


Fig. 5.6 Select a transformer

5.3.3.2 Enter Either MVA Increment or Enhanced Load Duration

As mentioned above, this application performs dynamic loading calculations for two different scenarios: (a) the fixed-duration maximum-step-load increment calculation and (b) the fixed-load-increment maximum-duration calculation. To perform a dynamic loading estimate, the user needs to enter either a desired load increment or desired load duration. When one option is entered, the other one will be disabled, as shown in Fig. 5.7. In consultation with engineers from SRP, the load increment is restricted to be no more than 1.5 per unit (42 MVA) for safety.

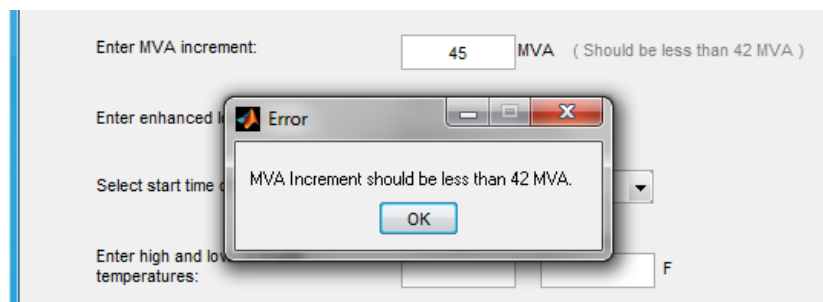


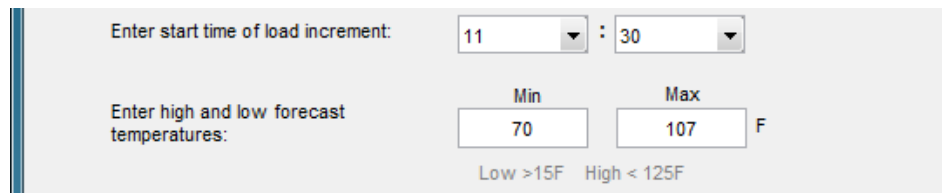
Fig. 5.7 Enter either MVA increment or enhanced load duration

5.3.3.3 Other Input

The remaining inputs, “start time of load increment” and “high and low forecast temperatures,” will be prefilled automatically by the program, as shown in Fig. 5.8. The

values for these fields are found as follows: After the user selects a transformer, the program reads in the real-time data file of that transformer, and uses the end time in that file as the prefilled start time. The user can change the start time using the drop-down box to the right of “Enter start time of load increment.” The program records the “high and low forecast temperatures” entered by the user each time they used the program. When the main interface is executed, the program will prefill those temperatures with the most recently entered values. The user can change “high and low forecast temperature” by retyping them.

As required by SRP, this application performs dynamic loading calculation for a period of 2-days (48-hour). If the “start time of load increment” entered by the user is earlier than the (prefilled) current time, it is assumed that the start time occurs in the second 24-hour period, since the start time for “today” cannot be earlier than today’s current time.



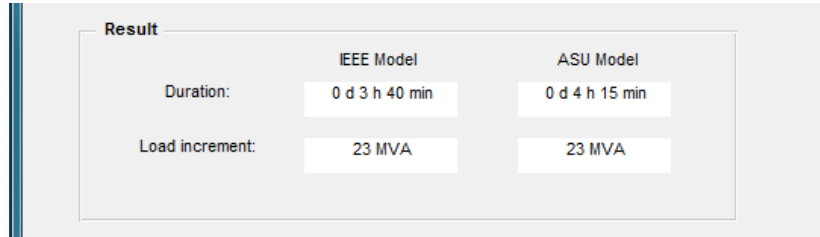
The screenshot shows a user interface with two main input sections. The first section is labeled "Enter start time of load increment:" and contains two dropdown menus with values "11" and "30" separated by a colon. The second section is labeled "Enter high and low forecast temperatures:" and contains two input boxes with values "70" and "107" followed by a unit "F". Below these boxes are the labels "Min" and "Max" and a note "Low >15F High < 125F".

Fig. 5.8 Other input

5.3.4 Output Area

When all needed information has been entered and vetted using the sanity-checks not described here, the dynamic loading calculation can be performed by clicking on the “Start” button. In this work, both IEEE and ASU models are used and give predictions respectively.

DLTA displays the dynamic loading calculation results including duration and load increment in both text and figures. The text message is displayed in the area labeled as “Result” in the main window. And, the figures are shown in the pop-up window.



	IEEE Model	ASU Model
Duration:	0 d 3 h 40 min	0 d 4 h 15 min
Load increment:	23 MVA	23 MVA

Fig. 5.9 Dynamic loading calculation results

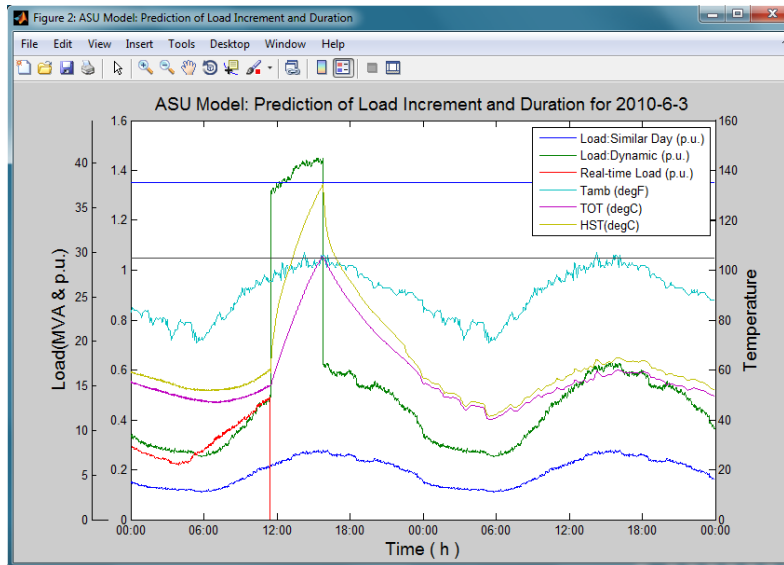
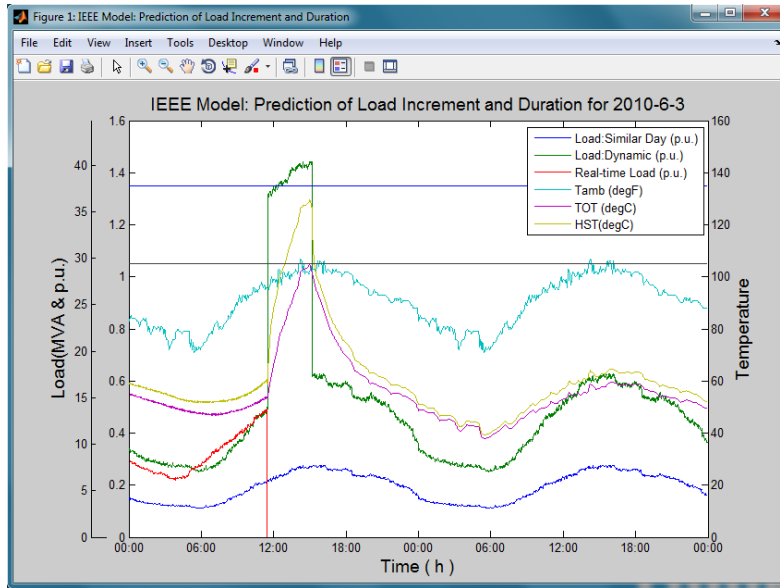


Fig. 5.10 Predicted load, TOT and HST curves

5.4 Conclusion

A detailed introduction to this application and graphical user interface design is provided in this chapter. The overall flowchart and salient functions are also presented.

CHAPTER 6

DYNAMIC LOADING ALGORITHM DESIGN

6.1 Introduction

This chapter focuses on the dynamic loading calculation, including the definition of dynamic loading, the dynamic loading algorithm, how to perform dynamic loading with selected models and the results of dynamic loading. Some examples on dynamic loading are provided. And some challenges in the algorithm design are also presented.

6.2 Definition of Dynamic Loading

Dynamic loading is the term used for loading (usually optimally) a transformer while taking into account the time variation of load, rule-of-thumb maximum allowable insulation temperatures, thermal time constants, cooling mode transitions, and ambient temperatures profiles. Because the load varies and the response of oil and insulation temperatures lag applied load, transformers can be loaded for a “short” time with a load greater than their name-plate rating.

When determining the loading capability of a transformer, the amount of load to switch on or off and for what length of time the transformer can be loaded above name-plate requires that the load, as a function of time, be forecasted and then the insulation temperature response to the load must be calculated via a differential equation numerically integrated inside a nonlinear optimization loop.

As mentioned in Chapter 5, two scenarios are considered for dynamic loading calculation in this application: fixed-duration maximum-step-load increment and fixed-load-increment maximum-duration. The maximum step-load-increment is defined as the

maximum load that can be added to a typical daily load curve for a desired time period that a transformer can sustain without violating HST or TOT thermal limits. The maximum-duration is defined as the longest period of time that a transformer can sustain a given step-change on a typical (or specified) daily load curve without violating HST and TOT thermal limits.

From a planning point of view, this information could be used in various ways. It could be used in reliability studies to calculate energy not served due to transformer outages or as guidelines to the system dispatchers to know how heavily they can load a transformer under emergency conditions.

6.3 Dynamic Loading Calculation for a 48-Hour Cycle

This section discusses how to perform dynamic loading calculations for a 48-hour cycle, which includes how to select “the most similar day” and the dynamic loading algorithm design.

The maximum dynamic loading calculation is an optimization problem with upper bound limited by the allowable peak HST/TOT thermal limits. The method is to multiplicatively scale up the base-case load shape to match the real-time data. The algorithm implemented by the application is described in detail below, and the corresponding flowchart is shown in Fig. 6.1.

1. Select “the most similar day” from the historical data file by using the forecast high and low temperatures. If no acceptable similar day is found, the user may select a “typical” day (in the “Typical Data” option).
2. Adjust the load profile and the ambient temperature profile of that selected day by

- multiplication, to match the end point of real-time data.
3. Make an initial estimation of the maximum step-load-increment (or the maximum duration), and update the load shape.
 4. Calculate the HST and TOT profile using this updated load profile and temperature profile, and check whether HST or TOT exceeds their thermal limits, respectively. If the maximum duration is larger than 24 hours, and both the HST and TOT do not reach their thermal limits, stop the iteration. In this case, the given step-load-increment is considered as can be sustained for an “unlimited” period.
 5. Use a Quasi-Newton method combined with a binary search algorithm to obtain the next estimate of maximum step-load-increment (or the maximum duration).
 6. Redo step 4 and step 5 until the limiting quantity (either TOT or HST lies within 1°C of its limit and the other is below its limit) is reached, or the loop runs 20 times without getting a solution.

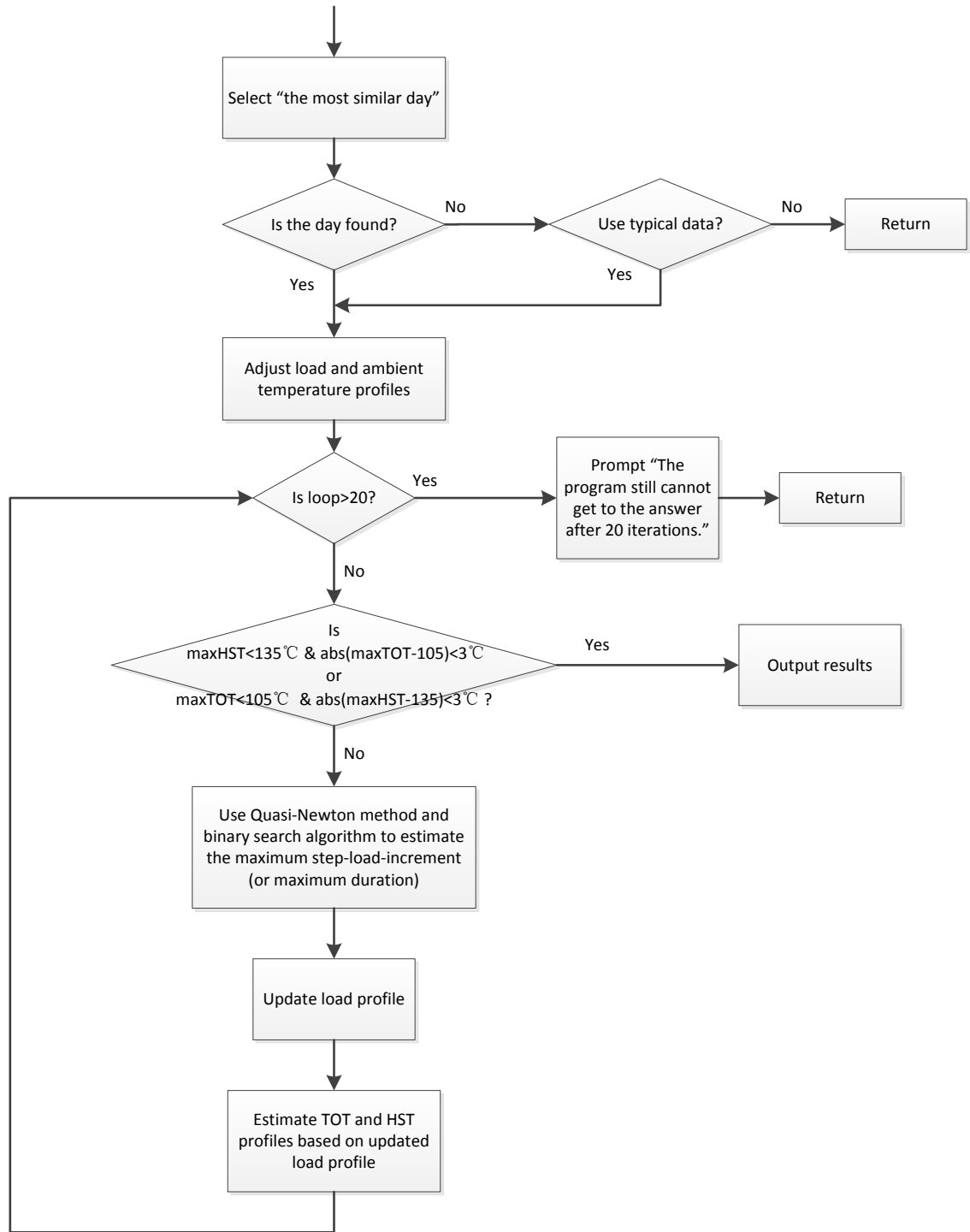


Fig. 6.1 The flowchart of dynamic loading calculation

6.4 Select “The Most Similar Day”

Since there is no way to easily estimate the real-time loading limit, one challenge that appears is to find proper load and ambient temperature profiles which could approximate the real-time data of the future.

In order to find a historical load profile which can best represent the real-time loading limit, the high and low forecast temperatures are used. It is assumed that, if the highest and lowest forecast temperatures for the day of interest are similar to those temperatures for another day in the historical record, the historical load profiles should be a good estimate of the profile for the day of interest. Therefore, the most similar day is selected by comparing all historical days’ high and low temperatures with the given forecasted value and calculating the a “closeness” metric using the following equation:

$$\Delta T = \min_i \left\| k_1 \left| T_{\min}^f - T_{\min,i} \right| + k_2 \left| T_{\max}^f - T_{\max,i} \right| \right\| \quad (6.1)$$

where

k_1, k_2 : are weighting coefficients

T_{\max}^f, T_{\min}^f : are the highest and the lowest forecast ambient temperatures

$T_{\max,i}, T_{\min,i}$: are the highest and the lowest ambient temperatures in the i th day of historical data

In consulting with SRP’s engineers, it was determined to set: $k_1 = 0.4, k_2 = 0.6$. If, using the above equation, $\Delta T > 5^\circ F$, then a message box will appear to warn the user that no similar day is found. At that point, the user is directed to select a “typical” day instead for dynamic loading calculation.

After “the most similar day” is found (or a typical day is selected by the user), the temperature profile will be scaled and adjusted to meet the input high and low forecasted value, as described in equation (6.2). The load profile is also scaled to meet the end point value of real-time load,

$$\begin{aligned}
 n &= \frac{T_{\max}^f - T_{\min}^f}{T_{\max} - T_{\min}} \\
 \Delta T_{adjust} &= T_{\max}^f - T_{\max} \cdot n \\
 T_{amb,new} &= T_{amb} + \Delta T_{adjust}
 \end{aligned} \tag{6.2}$$

where:

n : is the enlargement factor

ΔT_{adjust} : is the calibration temperature

6.5 Quasi-Newton Method and Binary Search Algorithm

Since the dynamic loading algorithm for those maximum-load and maximum duration scenarios is similar, only the first scenario (fixed-duration maximum-step-load increment) is used as an example to explain the algorithm design.

The step-load-increment estimation is conducted in two steps: first, an initial estimate of step load change corresponding to the maximum dynamic loading is made and then the estimate of the step load change is improved inside the iteration process.

Based on the scaled historical load profile, the start time of the load increment and the load increment duration, the first time the dynamic loading calculation subroutine is called, an initial guess of the step load increment is made. If the peak load of the forecast and scaled load curve is below 1.3 p.u., the initial estimate of step load increment is such

as to make the peak load equal 1.3 p.u. If the peak load is above 1 p.u., the initial estimate of the step-load increment is such as to increase the peak load by 50%.

During the iteration process, the subroutine makes corrections to the step-load-increment based on TOT/HST predictions. A Quasi-Newton method is applied here. The Quasi-Newton method assumes the relationship between step-load-increment and the temperature may be modeled as line with a slop and intercept. The slope is calculated by taking the numerical (rather than symbolic/analytic) derivative of load with respect to temperature using the equations below,

$$\begin{aligned}
 \Delta I_{oil}[k+1] &= \frac{\Delta I_{oil}[k]}{\max \theta_{oil}[k] - \max \theta_{oil}[k-1]} \cdot (TOT_{\max} - \max \theta_{oil}[k]) \\
 \Delta I_{hst}[k+1] &= \frac{\Delta I_{hst}[k]}{\max \theta_{hst}[k] - \max \theta_{hst}[k-1]} \cdot (HST_{\max} - \max \theta_{hst}[k]) \\
 \Delta I_{oil}[k] &= I_{oil}[k] - I_{oil}[k-1] \\
 \Delta I_{hst}[k] &= I_{hst}[k] - I_{hst}[k-1]
 \end{aligned} \tag{6.3}$$

where:

k : is the iteration index

I_{oil} : is the peak value of load curve estimated based on TOT

I_{hst} : is the peak value of load curve estimated based on HST

ΔI_{oil} : is the step-load-increment estimated based on TOT

ΔI_{hst} : is the step-load-increment estimated based on HST

In more detail of this process: first, we have two estimate of the operating points to calculate the first derivative, then, update the numerical estimate of the derivative using the most recent load and temperature iteration results. As the iterations proceed, the

estimation becomes more and more accurate and finally converges, meaning a load profile is reached with causes either the TOT or HST to hit its limiting value.

However, in our research it was found that some part of the peak HST/TOT versus step-load-increment curve (and also peak HST/TOT versus enhanced duration curve) has a slope that is close to zero, as shown in Fig. 6.2 and Fig. 6.3. Due to the sensitivity of the Quasi-Newton method for the zero (or shallow) sloped lines, a more complicated iteration procedure is needed.

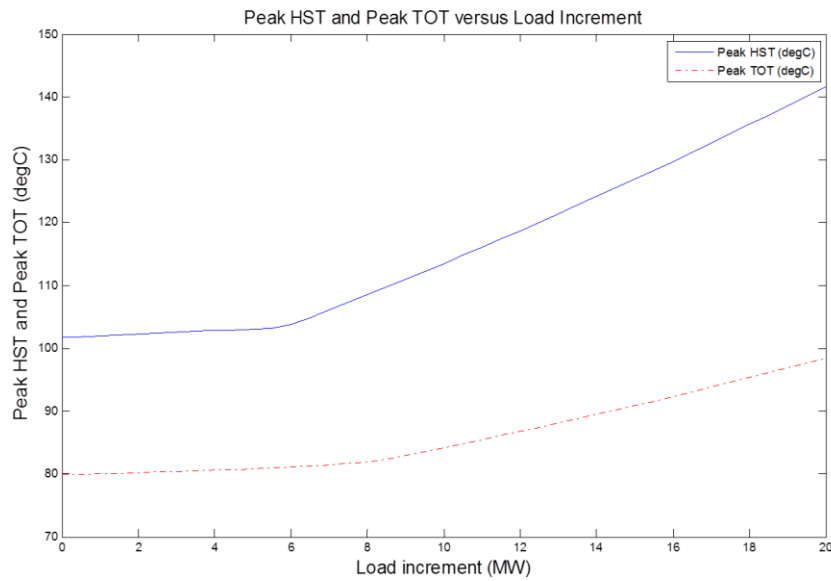


Fig. 6.2 Peak HST and Peak TOT versus Load Increment

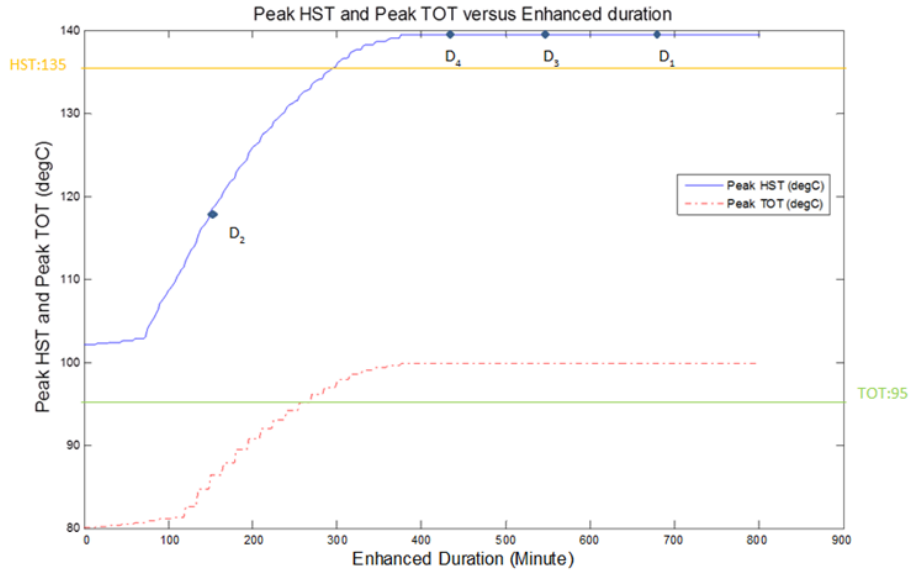


Fig. 6.3 Peak HST and Peak TOT versus Enhanced Duration

Usually, it takes 5-6 iterations to get the optimal solution by using Quasi-Newton method. However, if two adjacent estimates of load increment both lay on the part which the slope of the curve is close to zero (just like D_3 and D_4 in Fig. 6.3), the difference between the two corresponding peak TOT (or HST) values is nearly zero and, according to Equation (6.3), the inverse is unreasonably large; this causes the Quasi-Newton method to diverge.

To solve this problem, a binary search method is implemented. When the Quasi-Newton method diverges, the program will search the algorithms historical record of estimates and find the two specific adjacent estimates: the one causes the TOT or HST to be above its limit (“high” estimation, just like D_4 in Fig. 6.3) and the other that causes the TOT or HST to be below its limit (“low” estimation, just like D_3 in Fig. 6.3). Then, the binary search starts using these two estimates as the boundary points. In each step, the

algorithm creates a new estimate which is halfway between the “high” and “low” estimates. If the new estimation leads the TOT or HST being above its limit, the latest load estimate is set to be the new “high” estimate; if the new estimate leads the TOT or HST being below its limit, the latest load estimate is set to be the new “low” estimate. This process is repeated, until the maximum load is found whose corresponding TOT and HST values do not violate the specified limits. Typically, it takes 3-4 iterations to get the result by using the binary search. Based on SRP’s guidelines, the limiting value of HST is set to be 135 °C and the corresponding value of TOT is 105 °C. Once the TOT/HST limits are satisfied, the dynamic loading calculation is finished and the results are displayed on the user interface.

6.6 Cooling Mode Transition in the HST and TOT Calculations

As described in the previous section, as the load profile is updated (scaled) toward a maximum value during the iteration process, the HST and TOT profiles are correspondingly updated using the HST and TOT models introduced in Chapter 2

One challenge encountered is cooling mode or tier switching. When the transformer thermal performance is simulated using an updated load profile, the updated load profile changes the time at which the transformer enters into and exits each cooling mode. So the time point in the 48-hour simulation at which models are changed (to correspond to the appropriate cooling condition) must be recalculated during every loop.

6.7 An Example of Dynamic Loading Calculation for Broadway4 Transformer

As an example, a dynamic loading calculation is performed on the Broadway4 transformer. Fig. 6.4 shows the user input on the interface, and Fig. 6.5 and Fig. 6.6

display the estimate of the TOT/HST and load curve resulting from the dynamic loading calculation using the IEEE model and the ASU model, respectively.

The screenshot shows the TADL software interface with the following input parameters:

- Select a substation: Broadway
- Select a transformer: Broadway4-N60201010...
- Enter MVA increment: 23 MVA (Should be less than 42 MVA)
- Enter enhanced load duration: [Empty] Hours
- Select start time of load increment: 11 : 30
- Enter high and low forecast temperatures: Min 70, Max 107 F (Low >15 degF, High < 125 degF)

The results section shows:

	IEEE Model	ASU Model
Duration:	0 d 3 h 40 min	0 d 4 h 15 min
Load increment:	23 MVA	23 MVA

A "Dynamic Loading Calc" button is located at the bottom of the interface.

Fig. 6.4 Dynamic loading of Broadway4 transformer

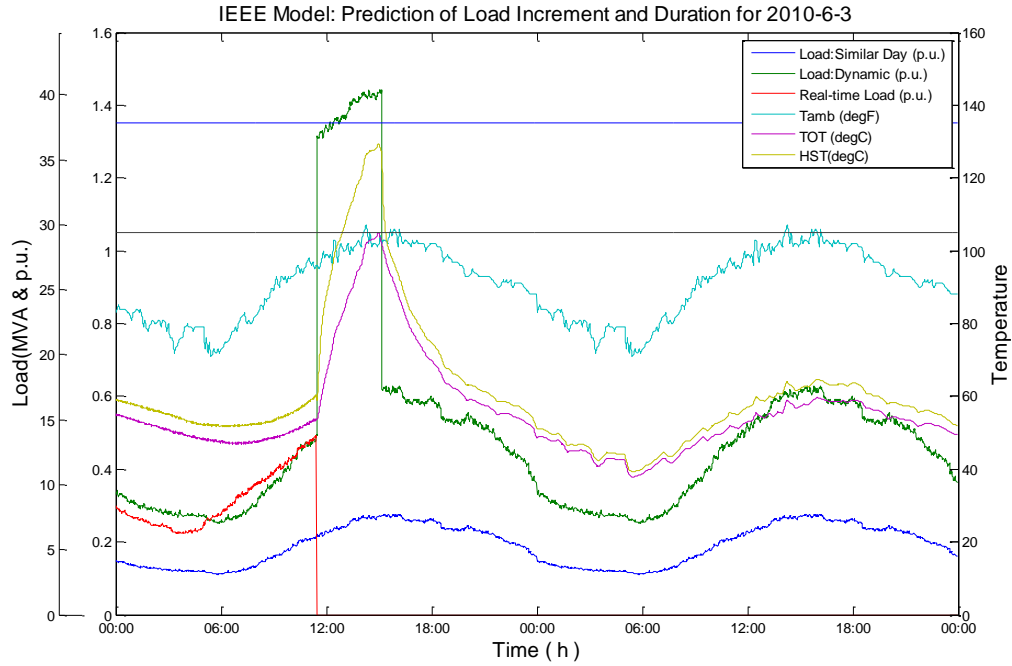


Fig. 6.5 Dynamic loading result of Broadway4 transformer using IEEE model

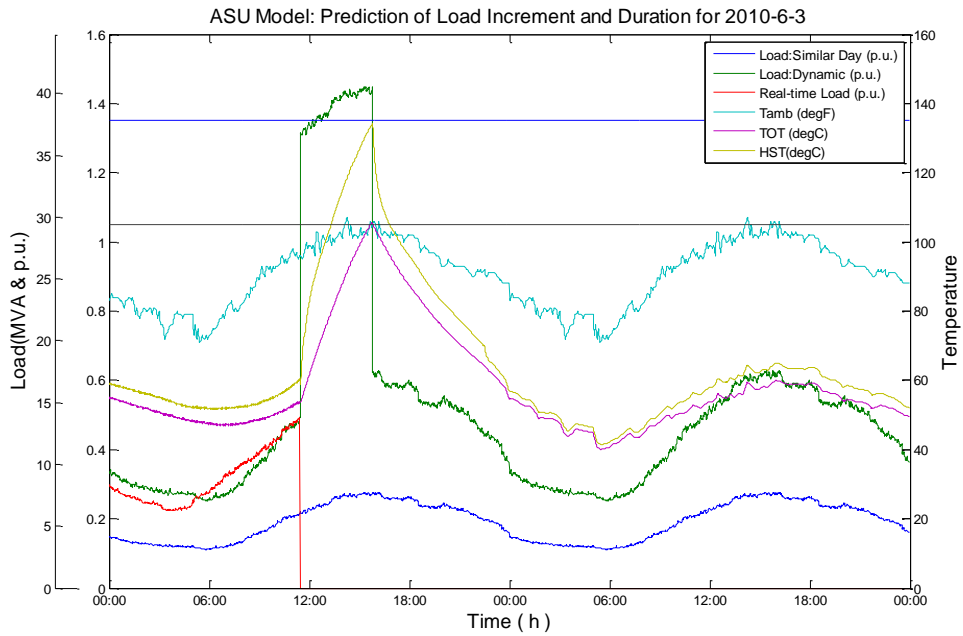


Fig. 6.6 Dynamic loading result of Broadway4 transformer using ASU model

6.8 Conclusion

The Quasi-Newton method combined with binary search algorithm is discussed in this chapter. It has been found through many (>100) trials that the combined methods have never failed to converge to an answer.

CHAPTER 7

CONCLUSIONS AND FUTURE WORK

7.1 Conclusions

The ultimate goal of this work is to produce a software-based application for transformers' dynamic loading calculation. In this document, two kinds of transformer thermal models, the IEEE TOT/HST models and the ASU TOT/HST models, are developed and analyzed in this work. Several metrics used to evaluate model acceptability in the previous work are described in Chapter 2, and later in Chapter 4, additional criteria used as an enhancement for model selection are introduced. Results of model testing on transformer Webber3 are discussed. Some researches to improve the model performance are also presented. Furthermore, the development of the new application based on the existing one and the GUI design are introduced. The dynamic calculation algorithm and some challenges encountered in the algorithm design are also discussed.

For this production grade application, both IEEE models and the ASU models are used. The advantage of the IEEE models is that all the parameters needed can be calculated from the heat-run test report. The ASU models are linearized models built from the measured data using linear regression. The ASU models are superior to the IEEE models in the fact that: 1) it incorporates ambient temperature variation into the model, 2) it creates a model that accurately represents what is in the field, and 3) it provides a measure of the reliability of the model.

Additional criteria such as the time constant and the model parameter K_3 are used, together with the existing metrics applied in the previous application, to determine the reliability of the ASU models. Results show that more consistent “good” model determination could be obtained if additional metrics were used.

The new application is developed by using an existing application, TTeMP, as a starting point. With an easy and simple graphical user interface, it is more convenient for the dispatchers and load specialists to use. It gets rid of all lengthy steps in TTeMP and gives results directly. Other enhancements are that it can work in a real-time environment and it has the capability to perform dynamic loading under emergency conditions, when there is a step change in the load curves. Mainly, two scenarios are considered for the dynamic loading calculation in this application: fixed-duration, get maximum-step-load increment; fixed-load-increment, get maximum-duration.

The Quasi-Newton method is applied in the dynamic loading calculation. Usually, it takes 5-6 iterations to get the optimal solution. However, it is found that under some circumstances, the Quasi-Newton method will diverge. Thus, a binary search algorithm is used as a backup when the Quasi-Newton method fails. Results show that it takes 3-4 iterations to get the optimal solution by using the binary search.

7.2 Future Work

This application needs some data files from an independent model building application. To develop that model building application and incorporate it with the dynamic loading calculation tool is the future work.

REFERENCES

- [1] O. A. Amoda, D. J. Tylavsky, G. A. McCulla, W. A. Knuth, "Acceptability of Three Transformer Hottest-Spot Temperature Models," *Power Delivery, IEEE Transactions*, vol. 27, no. 1, pp. 13-22, Jan 2012
- [2] O. A. Amoda, D. J. Tylavsky, G. A. McCulla, W. A. Knuth, "A new model for predicting hottest-spot temperature in transformers," *40th North American Power Symposium (NAPS)*, pp. 1-8, 28-30 Sep. 2008
- [3] Lida. Jauregui-Rivera, "Reliability Assessment of Transformer Thermal Models," Ph.D Dissertation, Arizona State Univ., Tempe, 2006.
- [4] D. J. Tylavsky, Mao Xiaolin, G. A. McCulla, "Data screening to improve transformer thermal model reliability," *North American Power Symposium*, pp. 560-568, 23-25 Oct 2005.
- [5] D. J. Tylavsky, Q. He, G. A. McMulla, J. R. Hunt, "Sources of error in substation distribution transformer dynamic thermal modeling," *IEEE Trans. Power Del.*, vol, 15, no. 1, pp. 178-185, Jan 2000.
- [6] IEEE Guide for Loading Mineral Oil Immersed Transformers, *IEEE Std. C57.91-1995*.
- [7] B. C. Lesieutre, W. H. Hagman, J.K. Kirtley Jr., "An Improved Transformer Top Oil Temperature Model for Use in an On-Line Monitoring and Diagnostic System," *IEEE Transactions on Power Delivery*, Vol. 12, No. 1, January 1997, pp. 249-256.
- [8] G. Swift, T.S. Molinski, and W. Lehn, "A Fundamental Approach to Transformer Thermal Modeling—Part I: Theory and Equivalent Circuit," *IEEE Transactions on Power Delivery*, Vol. 16, No. 2, April 2001, pp. 171-175.
- [9] G. Swift, T. S. Molinski, and W. Lehn, "A Fundamental Approach to Transformer Thermal Modeling—Part II: Field Verification," *IEEE Transactions on Power Delivery*, Vol. 16, No. 2, April 2001, pp. 176-180.
- [10] D. Susa, M. Lehtonen, and H. Nordman, "Dynamic Thermal Modeling of Power Transformers," *IEEE Transactions on Power Delivery*, Vol. 20, No. 1, January 2005, pp. 197-204.

- [11] L. Jauregui-Rivera, and D. J. Tylavsky, "Acceptability of Four Transformer Top-Oil Thermal Models—Part 1: Defining Metrics," IEEE Transactions on Power Delivery, Vol. 23, No. 2, April 2008, pp. 860-865.
- [12] L. Jauregui-Rivera, and D. J. Tylavsky, "Acceptability of Four Transformer Top-Oil Thermal Models—Part 2: Comparing Metrics," IEEE Transactions on Power Delivery, Vol. 23, No. 2, April 2008, pp. 866-872.
- [13] W. H. Tang, Q. H. Wu and Z. J. Richardson, "A Simplified Transformer Thermal Model Based on Thermal-Electric Analogy," IEEE Transactions on Power Delivery, Vol. 19, No. 3, July 2004, pp. 1112-1119.
- [14] L. W. Pierce, "An Investigation of the Thermal Performance of an Oil Filled Transformer Winding," IEEE Transactions on Power Delivery, Vol. 7, No. 3, July 1992, pp. 1347-1356.
- [15] L. W. Pierce, "Predicting liquid filled transformer loading capability," IEEE Transactions on Industry Applications, Vol. 30, No. 1, January/February 1994, pp. 170-178.
- [16] Xiaoping Su, Weigen Chen, Chong Pan, Qu Zhou, Li peng, "A simple thermal model of transformer hot spot temperature based on thermal-electrical analogy," High Voltage Engineering and Application (ICHVE), 2012 International Conference, pp. 492-495, 17-20 Sep. 2012
- [17] D. C. Montgomery, E. A. Peck, G. G. Vining, John Wiley and Sons, "Introduction to Linear Regression Analysis," 4th edition, New York, 2006
- [18] IEEE Standard for Standard General Requirements for Liquid-Immersed Distribution, Power, and Regulating Transformers, IEEE Std. C57.12.00-2006